



Cite this: *Environ. Sci.: Nano*, 2025, 12, 3821

## Exploring environmental nanobiogeochemistry using field-flow fractionation and ICP-MS-based tools: progress and frontiers†

I. A. M. Worms, \*<sup>a</sup> M. Tharaud, \*<sup>b</sup> R. Gasco, <sup>a</sup> M. D. Montaño, \*<sup>c</sup> A. Goodman, <sup>d</sup> V. I. Slaveykova, <sup>a</sup> M. F. Benedetti, <sup>b</sup> C. M. Churchill, <sup>f</sup> S. Fernando, <sup>\*f</sup> E. Alasonati, <sup>g</sup> C. Moens<sup>h</sup> and C. W. Cuss \*<sup>f</sup>

The recent application of sophisticated instrumentation and novel experimental techniques to environmental systems has driven the study of natural nanoparticles and nanoparticle systems towards new horizons. Moving beyond the detection of engineered nanoparticles in natural systems, these technologies create new knowledge about the composition, behaviour, and functions of natural nanoparticles as individual entities and particle systems. In this perspective article, we describe the progress and frontiers in this research area using case studies drawn from a range of published and unpublished data spanning diverse environmental systems. The companion paper *Exploring environmental nanobiogeochemistry using field-flow fractionation and ICP-MS-based tools: background and fundamentals* defines the emerging field of environmental nanobiogeochemistry and describes the fundamentals, optimization, advantages, and disadvantages of field-flow fractionation and ICP-MS-based techniques for advancing our understanding of natural nanoscale particles and particle systems. Thus, by combining the necessary background with the most recent findings and key challenges, these contributions provide key knowledge for new and established researchers entering this exciting field and lay the groundwork for future research.

Received 24th January 2025,  
Accepted 3rd July 2025

DOI: 10.1039/d5en00096c

rsc.li/es-nano

### Environmental significance

The use of field-flow fractionation and ICP-MS-based techniques to study natural nanoparticles (NNPs) is hindered by challenges in their operation and interpretation of the corresponding data, potential artefacts arising from the nature and complexity of environmental systems, and lack of understanding about the knowledge they can provide. However, recent advancements have opened research frontiers that can substantially improve the understanding of NNP composition, behavior, and functions. This perspective article identifies the frontiers and challenges in understanding natural nanoparticle systems using published and unpublished studies applying these techniques in soil, aquatic and biological systems; economic geology; and standardization. Combined with the companion tutorial review *Exploring environmental nanobiogeochemistry using field-flow fractionation and ICP-MS based tools: background and fundamentals*, this perspective article provides the tools and knowledge for new and established researchers to advance the emerging field of environmental nanobiogeochemistry.

## 1. Introduction

Natural nanoparticles (NNPs) are a subset of aquatic colloids, which play critical roles in environmental systems owing to their small size, diverse composition, and large surface area, facilitating the adsorption and transport of contaminants and nutrients.<sup>1–3</sup> Their complex behavior is influenced by their agglomeration, settling, and fractal structures and is not fully understood to date.<sup>4</sup> Although advances in nanotechnology have improved the characterization of engineered nanoparticles (ENPs), the diversity and polydispersity of NNPs challenge traditional methods and models. A process-based approach integrating advanced analytical techniques such as field-flow fractionation (FFF) and inductively coupled plasma mass spectrometry (ICP-MS) has emerged as a powerful tool for studying NNPs.<sup>5,6</sup> These techniques enable the minimally

<sup>a</sup> Département F.-A. Forel des sciences de l'environnement et de l'eau, Université de Genève, Switzerland. E-mail: isabelle.worms@unige.ch

<sup>b</sup> Université Paris Cité- Institut de Physique du globe de Paris, CNRS, F75005 Paris, France. E-mail: tharaud@ipgp.fr

<sup>c</sup> Western Washington University, Bellingham, USA. E-mail: montanm2@wwu.edu

<sup>d</sup> Biophysicochimie des systèmes biologiques et environnementaux, Université de Montréal, Canada

<sup>e</sup> Colorado School of Mines, Golden, USA

<sup>f</sup> Laboratory for Environmental and Analytical Nanogeochemistry, Memorial University of Newfoundland (Grenfell Campus), Canada.

E-mail: ksuffernand@mun.ca, ccuss@mun.ca

<sup>g</sup> Laboratoire National de Métrologie et D'Essais, Paris, France

<sup>h</sup> Soil and Water Management, KU Leuven, Belgium

† Electronic supplementary information (ESI) available. See DOI: <https://doi.org/10.1039/d5en00096c>



invasive separation and detailed elemental analysis of NNPs, providing insights into the cycling of NNPs and their environmental impacts. Recently, they have been applied to the nanogeochemical environment to better understand the properties and dynamics of natural particles and colloids at the nanoscale.<sup>7,8</sup> The coupling of asymmetric flow FFF (AF4) with ICP-MS for online analysis and the use of ICP-MS in the single-particle mode (spICP-MS) have become especially valuable for advancing environmental nanobiogeochemistry.<sup>9,10</sup> The more recent addition of a time-of-flight (TOF) mass analyzer to spICP-MS facilitates multi-elemental analysis of each of the hundreds of thousands to hundreds of millions of nanoscale particles and colloids that are present in each liter of most natural waters.<sup>7,8,11,12</sup>

Combined, AF4-ICP-MS and spICP-(TOF)MS have led to substantial advancements in the field of environmental nanobiogeochemistry, which seeks to characterize the range of natural nanogeochemical systems, their dynamics, their roles in ecosystem functions, and the impacts of disturbances. The present perspective is accompanied by a first part tutorial review entitled *“Exploring environmental nanobiogeochemistry using field-flow fractionation and ICP-MS-based tools: background and fundamentals”*, which highlights the fundamentals and recent advancements of these methods for their use in environmental nanobiogeochemistry. It also provides technical background about these analytical methods, including their advantages, optimization, and limitations.

The present companion perspective highlights key historical and recent studies that lay the groundwork for environmental nanobiogeochemistry using AF4-ICP-MS and a range of ICP-MS-based methods, organized according to their environmental milieu. These highlights integrate published results with more recent unpublished case studies to demonstrate the key advancements, challenges and future research in this nascent field, with a focus on the sampling, characterization and analysis of NNPs, and the dynamics of the associated TEs. The challenges related to the standardization of analytical and data treatment processes and artefacts in the sampling of systems of nanoparticles and colloids (NPs) are also discussed. As a whole, this work seeks to delineate the frontiers in nano-analysis for addressing the mechanisms leading to NPs stability or perturbation, thus establishing the relevance of NPs and connecting their measurement to potential impacts at the nanoscale, mesoscale, ecosystem scale, and global scale, setting the stage for future interdisciplinary research using these and other multi-method approaches.

## 2. Historical and recent progress in the application of AF4 and ICP-MS-based tools for the characterization of NPs

### 2.1. Soil systems

The soil provides critical ecosystem services such as buffering, nutrients, and sequestration of carbon and toxic substances. It

acts as a biogeochemical reactor where nutrients and contaminants are transformed, sequestered, or released due to various physical, chemical, and biological processes.<sup>13</sup> These processes primarily occur at the solid–water interface or on the surface of organic and mineral compounds. Therefore, the potential reactivity of soil depends on the specific surface area of these compounds, which provide interfaces for sorption/partition, precipitation, volatilization, oxidation/reduction, and complexation. The natural nanoparticle system (NPs) in soils is composed of various NNPs such as organic substances such as humic and extracellular polymeric substances (HS and EPS), together with inorganic nanominerals such as (hydr)oxides of iron, aluminum, or manganese, aluminum-silicate clays, and metal sulfides. The solid–water interface created by these NNPs plays a crucial role in governing the concentrations and speciation of most reactive trace elements (TEs) and many pollutants.

**2.1.1. Soil structure and colloidal mobilization.** Colloidal organo-mineral associations are part of the immobile soil phase and contribute to the formation of microaggregates. Several beneficial soil functions such as C sequestration, nutrient retention, and aeration are linked with the structure and composition of soil aggregates, which according to their size follow the order of macroaggregates ( $>250\text{ }\mu\text{m}$ ) composed of large ( $250\text{--}20\text{ }\mu\text{m}$ ) and small ( $20\text{--}2\text{ }\mu\text{m}$ ) soil microaggregates (SMA), and organo-mineral associations  $<2\text{ }\mu\text{m}$ , called composite building units.<sup>14</sup> Furthermore, the composite building units contain soil colloids with a size of  $<1\text{ }\mu\text{m}$ . Hence, better understanding of the soil structure and aggregate stability requires the further examination of the composition of the colloidal and nanosized building blocks of aggregates.

The majority of AF4 studies on environmental soil samples use UV absorbance (typically at 254 nm) for the detection of organic carbon. Nischwitz *et al.*<sup>15</sup> developed carbon detection online with AF4 using ICP-MS, initially for fine particulate carbon in aqueous samples. This was shown to be feasible for the quantification of larger and more robust carbon-based structures such as charcoal-spiked soil particles with sizes of up to 450 nm.<sup>16</sup> Although the detectable concentrations are still relatively high compared to that of nanoscale OM, this methodology has the advantage of simultaneously analyzing carbon and other nutrients *via* ICP-MS. Alternatively, AF4 can be coupled online with an organic carbon detector (OCD), which is based on a thin film UV-reactor that oxidizes organic carbon and detects  $\text{CO}_2$  by infrared.<sup>15</sup> Organic carbon detection with an OCD detector coupled to AF4-ICP-MS was also used to characterize colloidal P carriers in soil.<sup>17,18</sup> Total organic carbon (TOC) has also been measured on collected NNP fractions after AF4 fractionation to characterize colloidal uranium in soil.<sup>19</sup> To improve fraction collection for further offline characterization, Nischwitz *et al.*<sup>20</sup> recently used a commercially available preparative AF4 channel for the offline detection of charcoal in soil extracts with gas chromatography and a flame ionization detector.

Several studies characterized the fine colloidal fraction from soil aggregates in arable Luvisols using AF4-ICP-MS



with OCD to determine how colloidal iron and organic carbon control soil aggregate formation and stability as cementing and glueing agents, respectively.<sup>21–23</sup> Colloid characterization was accompanied by mechanical (ultrasound) and chemical (removal of Fe-oxides and removal of OC) disintegration and subsequent regeneration of macro-aggregates,<sup>22</sup> and the addition and removal of colloids from micro-aggregates. This was evaluated for soils under different management systems (cropped and bare fallow), which affected the soil structural properties.<sup>21,23</sup> Moreover, AF4 and pyrolysis-field ionization mass spectrometry were used to compare the composition and stability of colloid-associated OM in both free colloids (*i.e.* potentially mobile water-dispersible) and occluded colloids (*i.e.* building units of soil microaggregates).<sup>24</sup> Free colloids were dispersed in water suspensions during wet-sieving, while occluded colloids were released from water-stable aggregates by sonication. The free and occluded fine colloids were predominantly present as organo-mineral associations, with the free colloids relatively enriched with constituents of less decomposed plant residues. Alternatively, the occluded colloids contained more microbial decomposition products with a higher stability against further decomposition or mineralization.

**2.1.2. Collection of soil solutions, extraction and characterization of NNPs.** The methods for collecting soil solutions have different extraction efficiencies for NNPs, yielding a large variation in the estimated concentrations of mobile elements. Collecting samples of mobile NNPs in soil is also challenging due to their retention in the sampling devices and changes in *in situ* conditions given that extraction affects the pH and ionic strength, and hence colloidal characteristics.

Recent AF4 studies commonly focused on water-dispersible colloids (WDC), including NNPs, that are easily dispersible on contact with soil and water.<sup>25–27</sup> As rainfall or irrigation contributes to the release and transport of WDC, they are considered indicators for mobile soil colloids. However, solid extraction with water has low ionic strength compared to pore water from unsaturated soils. Thus, water extracts disrupt the aggregates that release colloids and dilute the polyvalent cation concentrations that otherwise flocculate colloids, resulting in high colloidal concentrations. Du *et al.*<sup>28</sup> used AF4-UV-ICP-MS to quantify the distribution of TEs between small, simple complexes and colloid-associated forms in soils extracted using different procedures. In water extracts, a greater proportion of TEs was associated with dissolved organic matter (DOM) and/or inorganic NNPs, although water extracts generally also liberated more small and simple TE-bearing complexes than observed for 0.01 M CaCl<sub>2</sub> extract. Likewise, Bergen *et al.*<sup>29</sup> found that 0.01 M CaCl<sub>2</sub> extracts underestimated mobile U compared to *in situ* pore water obtained with centrifugation due to colloid aggregation at higher Ca concentrations. In contrast, the Cd concentration in 0.01 M CaCl<sub>2</sub> extracts exceeded that of pore water due to the chloride complexation and higher Ca, mobilizing Cd. AF4-UV-ICP-MS analysis of the

pore water revealed the co-elution of U with colloidal organic matter, oxyhydroxides, and aluminosilicates (*i.e.* clays), illustrating the colloidal transport of U by these vectors. In the context of measuring long-term U and Cd leaching from agricultural soils, soil leaching experiments with undisturbed soil columns in a laboratory better indicate potential leaching losses in the field than a single pore water composition of field-moist soil extracted *via* centrifugation. This is because the former yields the time-integrated data provided that suction plates and/or bottom filters are analyzed to account for the colloids retained at the bottom of the columns.<sup>29</sup> However, care must be taken to account for edge effects in soil columns, wherein liquid migrates down the column differently at the edges when in contact with the container holding the soil.

Stronger extractants have also been used to release soil NNPs for AF4-UV-ICP-MS analysis. Regelin *et al.*<sup>30</sup> used Na<sub>2</sub>CO<sub>3</sub> and Na<sub>4</sub>P<sub>2</sub>O<sub>7</sub>, finding that the latter could also disperse considerable amounts of organo-mineral aggregates. Their rationale was that the dispersion of colloids from soils due to changes in solution chemistry is the most common source of colloids in soils and groundwater. Loosli *et al.*<sup>31</sup> evaluated the potential of several extractants (NaOH  $\leq$  Na<sub>2</sub>CO<sub>3</sub>  $<$  Na<sub>2</sub>C<sub>2</sub>O<sub>4</sub>  $<$  Na<sub>4</sub>P<sub>2</sub>O<sub>7</sub>) to disperse NNPs from soil samples to facilitate their characterization. Among them, the Na<sub>4</sub>P<sub>2</sub>O<sub>7</sub> dispersant had the highest colloidal recovery and extracted NNPs with a narrower size distribution relative by inducing the breakup of soil micro-aggregates, reducing free multivalent cation concentrations in soil pore water by forming metal-phosphate complexes, and enhancing the surface charge *via* phosphate sorption on the nanoparticle surfaces.

Minimal disturbance is expected from the *in situ* collection of percolating water in the field using lysimeters with large pore sizes. To avoid limitations due to TE contamination from conventional lysimeters, a new lysimeter with a 5  $\mu$ m pore size was constructed entirely of 316 L surgical SS for collecting soil solutions under vacuum pressure. This system was used to obtain the TE distributions amongst major colloidal forms in solutions collected from saturated soils using AF4-UV-ICP-MS.<sup>32</sup>

**2.1.3. TE size-based distribution in soil using AF4-UV-ICP-MS.** The dissolved fraction (*i.e.*  $<0.45$   $\mu$ m by filtration) of TEs in soil pore water and other aquatic settings is generally considered to be the most mobile, bioaccessible, and bioavailable. The elements in this fraction can be present as molecular species, simple complexes, or associated with NNPs, each having different mobility and bioavailability. Measuring the abundance and size distribution of dissolved TE species is challenging due to their small size, variability in size distribution, chemical diversity (organic and inorganic material such as macromolecules, humic substances, oxyhydroxides, and small phyllosilicate clays), and stability.<sup>33–35</sup>

Depending on the conditions applied for fractionation in AF4, the size-selectivity of the NNPs can be varied to favor the resolution of smaller or larger NNPs, as illustrated in the two cases studies below (Fig. 1 from 300 Da to approx. 20 nm;



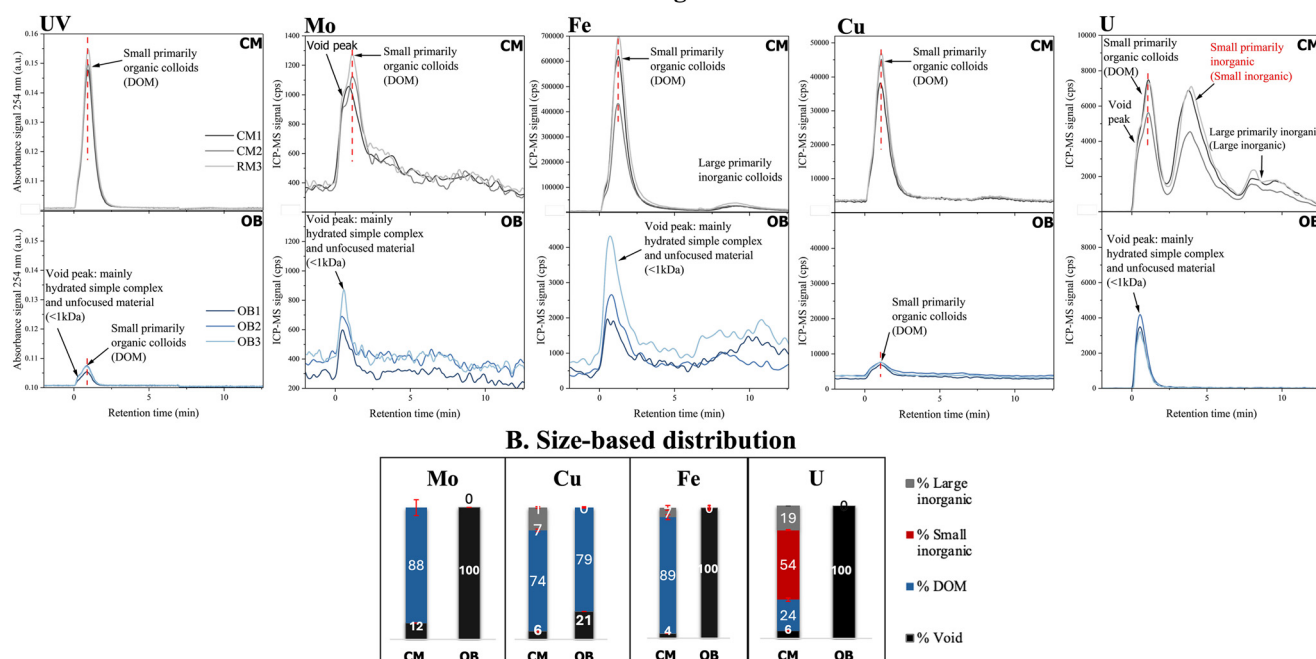


**Fig. 1** (A) Absorbance and ICP-MS fractograms and (B) size-based distributions (%) of dissolved Cu, Fe, Mo, and U > 300 Da obtained by AF4-UV-ICP-MS for selected elements contained in two filtered (<0.45  $\mu$ m) soil solutions (CM and OB soils). CM1, CM2, CM3, OB1, OB2, and OB3 refer to triplicates; CPS: counts per second (unpublished data).

and Fig. 2 from 1 nm to 100 nm). The calibration of both AF4 and ICP-MS is a key aspect of ensuring reliable analysis and discussed in the companion publication, *Exploring environmental nanobiogeochemistry using field-flow fractionation and ICP-MS based tools: background and fundamentals*.

The ability of the combined AF4-UV-ICP-MS technique to compare the lower end of the size distribution of NNP and TEs concentrations within this pool, including small organic-dominated (*i.e.* humic substances) and larger primarily inorganic NP, is first illustrated (Fig. 1) using forage-grown agricultural soil from Cormack in Newfoundland, Canada (CM soil), and overburden soil from the Alberta Oil Sands Region in Alberta, Canada (OB soil). Based on the particle size distribution, the CM soil was classified as loam, while the OB soil was classified as sandy clay loam. The soil solution characteristics, sample collection, and AF4-ICP-MS analytical parameters are detailed in section S1.<sup>†</sup> The relative DOM quantity, estimated using absorbance at a wavelength of 254 nm, was markedly higher in CM than in OB soil solutions. This higher DOM content in CM soil accounts for the greater DOM-associated peaks of most elements (dashed line in Fig. 1A). The presence of Mo and U solely in the void peak of OB soil solutions suggests elevated lability and mobility, likely as hydrated ions and other small, simple complexes (Fig. 1B). The void peak may also contain unfocused materials, such as large colloids eluted in steric mode. However, the disappearance of the void peak with an extended focusing time suggested that these materials were not large colloids eluting under steric inversion (data not

shown). Both soils indicated a high affinity of Cu for DOM. Trace elements such as Fe and Cu were predominantly in forms with generally lower lability (*i.e.* DOM-associated and primarily inorganic) than U or Mo in both soils. Noteworthy, it is expected that the TEs associated with colloids in AF4 are relatively non-labile due to labile ions desorbing from colloids and passing through the membrane during continuous re-equilibration with the metal-free carrier fluid at the focusing position; however, this assumption has not been rigorously tested. Uranium in the CM soil was distributed across four different types of nano-colloids, with intermediate-sized primarily inorganic species, which were not observed in the Fe size distribution (Fig. 1, red).

Potentially toxic TEs can be associated with either humic substances or NNPs depending on their relative affinities, as revealed for As, which had a similar size distribution to Fe in 3 types of soils (Fig. 2). These soils differ in their pH, organic carbon (OC) and aluminosilicate content. Fig. 2 additionally illustrates how NPS fractionation for a size distribution of <100 nm in the pore water helps in estimating the nature of iron-based NNPs using both UV detection and ICP-MS elemental composition. As discussed in ESI,<sup>†</sup> section S2, different types of NNPs can be associated with different size ranges. For instance, iron (and Al) can be found as stable chelates with humic substances at the lower size end of the fractograms (<5 nm), coeluting with Cu complexes and UV absorbance, as observed for Rhy and Alu soils. The increase in Fe-containing NNP size is attributed to the oligomerization process of Fe,<sup>37</sup> which does not coelute with the UV signal for sizes <5 nm (Zeg soil), forming small NNPs.<sup>36</sup> These NNPs tend to grow and

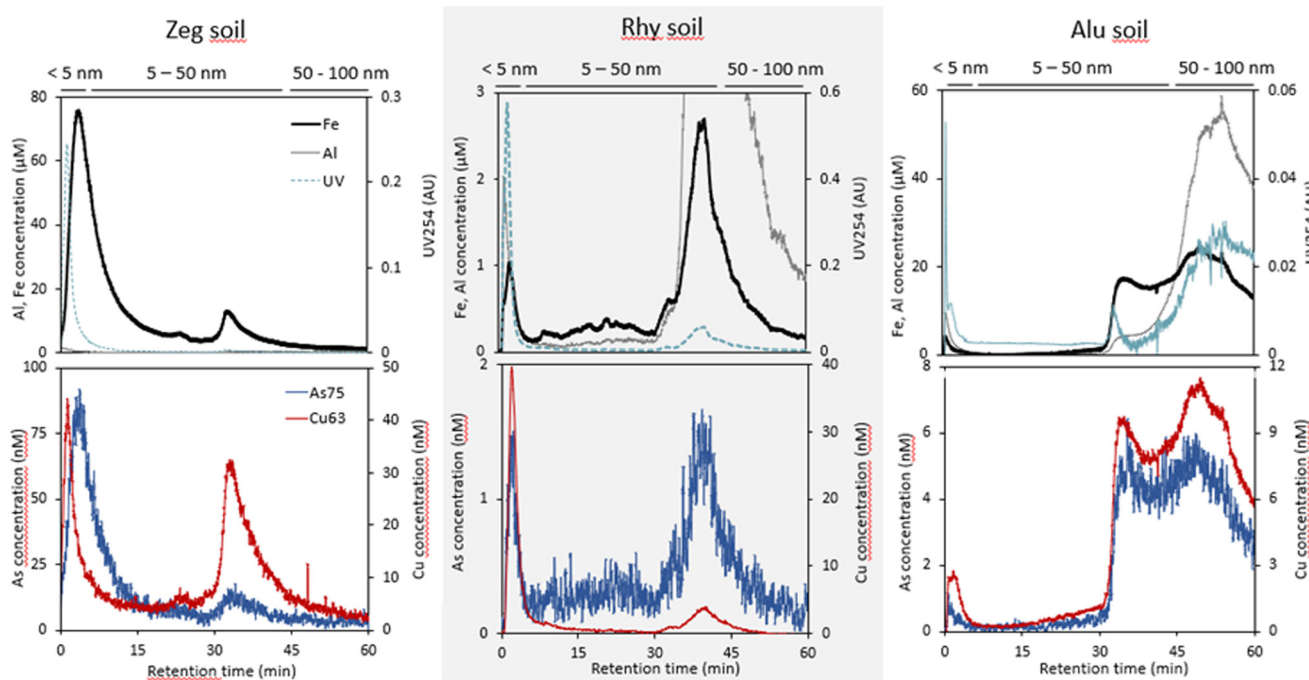


**Fig. 2** Size-resolved analysis of NPs (<100 nm) using AF4-UV-ICP-MS of pore water from three soils (Zeg soil, pH 5.5, 3.5% OC; Rhy soil, pH 5.2, 12% OC; Alu soil, pH 5.8, 0.9% OC). Size and composition analyses reveal mono-nuclear Fe- and Al-containing OC complexes (Rhy and -Alu soils) or Fe oligomers with sizes <5 nm (Zeg soil) and larger, predominantly inorganic colloids consisting of illite clay and Fe oxyhydroxide-clay associations (see discussion in ESI† section S2). Trace elements (e.g. Cu and As) co-eluted with the humic substances and NPs, indicating their role as vectors of TEs in the environment. From left to right, the fraction of Fe with sizes in the range of 50–100 nm increases, which was related to the soil organic carbon content based on AF4-UV-ICP-MS analysis of pore water from 11 soils.<sup>36</sup> It should be noted that the size distribution of As follows that of Fe. Fractionation conditions and settings are provided in ESI† section S2. Part of the data are taken from previously published work,<sup>36</sup> whereas the TE data have not been published previously.

heteroaggregate upon a decrease in OC content<sup>38</sup> (Rhy and Alu soils), leading to an apparent increase in the size of Fe-containing NPs fractionated in the range of 5–50 nm. The presence of aluminosilicate, evidenced using the Si/Al and Si/Mg ratio,<sup>39</sup> on which iron oxides can adsorb, further increased the apparent size (50–100 nm and above) obtained for Fe-containing NPs, as observed for Alu soil.

AF4-ICP-MS clearly advances our ability to access the size, potential nature and associated concentration of TEs within the NPs in soils.<sup>32,36,38,40,41</sup> The examples shown above illustrate the use of AF4-ICP-MS for measuring the colloid association of TEs by small NPs, which are potentially more mobile and reactive than particles.

Several environmental conditions release or are point sources for the dynamic formation of small organo-mineral colloids in soil pore water. For instance, redox processes induce changes in the aqueous composition and transformation of the solid-phase matrix, which can generate (in)organic colloids both in anoxic and oxic environments and where oxic/anoxic transitions exist, such as floodplains, wetlands, peatlands, and paddy soils.<sup>42</sup> Recent studies have also used AF4-ICP-MS to study the redox-driven changes in colloid contribution, NNP composition, and TE size distribution in paddy soils related to arsenic,<sup>43</sup> metals,<sup>44</sup> and carbon cycling,<sup>45</sup> and in floodplain soils polluted with high levels of mercury.<sup>46</sup> The characterization of suboxic/anoxic environmental samples requires careful

sampling and analysis protocols to preserve the native redox status of the targeted elements. Concerning AF4 analysis, measures to ensure oxygen-free conditions included using N<sub>2</sub> (ref. 43 and 44) or Ar (ref. 45 and 47) for flushing solvents and syringes, rinsing bottles, and degassing the carrier solution.<sup>33–35,40,41</sup>

**2.1.4. Further considerations for combining with spICP-(TOF)MS.** Currently, spICP-MS analysis offers an important advantage over AF4-ICP-MS for characterizing TE-bearing NPs at low concentrations. For instance, spICP-MS analysis combined with XAS analysis to determine mineralogy allowed the detection of metacinnabar (Hg) colloids in mining-impacted soil.<sup>48</sup> Characterizing the stoichiometry of individual colloid particles with single-particle ICP-(TOF)MS could combine these methods to better understand NPs in soils and soil solutions, and the interactions between different types of NPs. Likewise, the nature of Si-bearing NP extracted from soil and analyzed with ICP-TOFMS on a single-particle basis identified aluminosilicate NPs containing Si, Al, and other elements in varying proportions, in addition to mono-metal Si-containing NPs, presumably SiO<sub>2</sub>.<sup>49</sup> Dual-analyte spICP-MS also allowed the discrimination of two typical soil nanoparticles, kaolinite and goethite, based on the elemental ratios measured in single NPs.<sup>50</sup> spICP-TOFMS has also been applied to distinguish engineered from natural Ti-containing NPs in soil based on differing elemental ratios.<sup>51</sup> Finally, spICP-TOFMS has recently

been combined with machine learning to successfully characterize the stoichiometry of CuS, Cu<sub>2</sub>S, and CuFeS<sub>2</sub> with 75–99% accuracy.<sup>52</sup>

Taken together, AF4-ICP-MS and spICP-(TOF)MS enable the in-depth characterization of certain aspects of the nanobiogeochemistry of the soil environment, including the structure of soil microaggregates, their stability, the generation of NNPs, their release in soil solution, and their interactions and roles as nanovectors facilitating TE transport. Future works should compare these findings with studies of uptake to measure the relationships between the forms of these elements and their lability, especially in the smallest components of NPs. This information will also be useful for developing models to predict the mobility and bioaccessibility of TE in different soil

types, aiding in environmental risk assessments, the development of soil remediation strategies, and the provision of nutrients in agriculture. As depicted in this section, the challenges associated with preserving the natural size distribution and speciation of NPs during the collection of soil pore water is an active area of development.

## 2.2. Aquatic systems

Previously, individual NNPs and their associated NPs in aquatic systems have been the most common focus for characterization using AF4-ICP-MS and spICP-(TOF)MS. Beginning with small-scale proof-of-concept studies in aquatic systems rich in organic matter and colloids, or using ENPs,<sup>53–57</sup> these analyses have

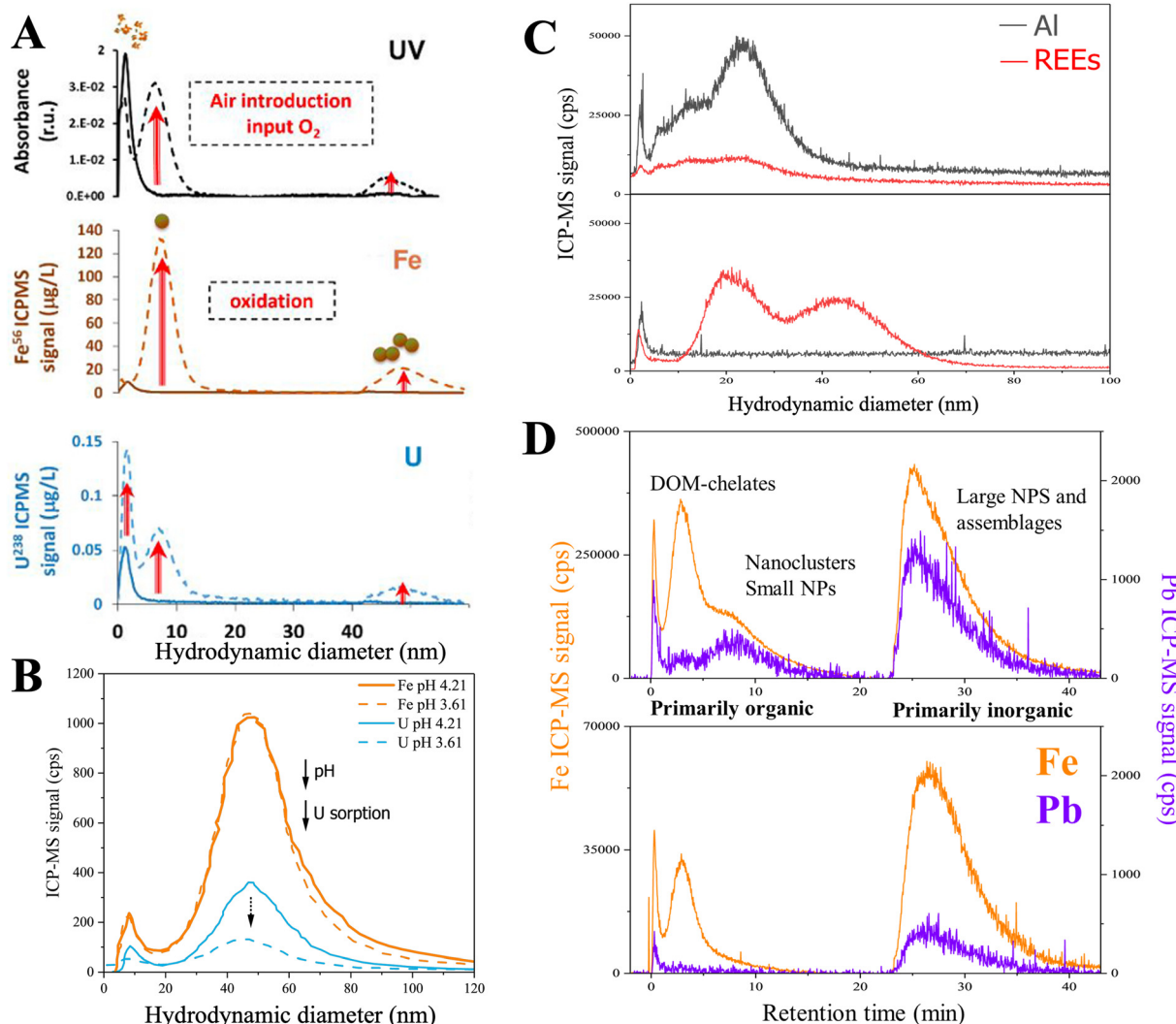


**Fig. 3** Multi-scale and multi-scope demonstration of AF4-ICP-MS capabilities for investigating preferential TE association within aqueous NPs. A) Impact of iron oxidation and small (<10 nm) Fe-containing NP generation on uranium size distribution and mobility in wetland water<sup>47</sup> and B) impact of pH on UO<sub>2</sub><sup>2+</sup> adsorption on synthetic ferrihydrite;<sup>84</sup> (reproduced with permission from the American Chemical Society). C) Acidic groundwaters at an industrial site with elevated levels of REEs; nanoparticulate REEs in the operationally defined “dissolved” fraction were associated with Al in some samples, suggesting adsorption on clays or (oxy)hydroxides<sup>66</sup> (reproduced with permission from Elsevier). D) Natural nanoparticles in boreal rivers, where Fe and Pb existed as DOM-chelates, nanoclusters/small nanoparticles, and larger assemblages differing with spatial, temporal, and hydrodynamic factors.<sup>7</sup>



evolved to measure trace concentrations in typical rivers and lakes,<sup>58–63</sup> low-oxygen groundwaters,<sup>64–66</sup> and to characterize NPS processes and properties across different scales (Fig. 3).<sup>7,67–69</sup> The following section provides an overview of the wide range of NPS properties and processes in these and other aquatic systems that have recently been characterized using these methods, while also identifying challenges and frontiers for future research.

**2.2.1. Composition of NPs in aquatic systems.** The use of AF4-ICP-MS to quantitatively measure the composition of NPS in streams and river systems can be considered a robust methodology. Consequently, recent trends have shown a shift from the proof-of-concept aspect towards a scale-up in the number of samples to improve the understanding of large-scale environmental processes and geochemical cycles involving colloids by monitoring colloid size, composition, and concentration at larger spatiotemporal scales.<sup>21,61,68–70</sup> For instance, the NPS of European forest stream waters were studied in 96 samples, covering 2 large transects in Europe.<sup>71</sup> The size and composition of stream water NPs and colloids varied across Europe from North to South, changing from Fe- to Ca-dominated particles, together with associated changes in acidity, dominant lithology, and type of forest. Organic-rich components of small size were associated with a large quantity of Al and some Fe and Mn, most probably composed of HS combined with small oxyhydroxides ( $d_h < 20\text{--}25\text{ nm}$ ). An intermediary size fraction of  $20\text{--}25\text{ nm} < d_h < 60\text{--}70\text{ nm}$  characterized by the presence of Ca and Mn even under acidic conditions contributed a significant proportion of the NNP found in the south of Europe.<sup>71</sup> Clay minerals with  $d_h = 60\text{--}70$  to  $\sim 400\text{ nm}$  and most probably held together by oxides and stabilized by organic matter were identified in all streams.<sup>71,72</sup> Using an online OCD, the average composition of NPs  $< 450\text{ nm}$  measured in European stream waters was reported to be  $53\% \pm 21\%$  Fe,  $50\% \pm 26\%$  P,  $26\% \pm 29\%$  Mn,  $41\% \pm 24\%$  Al,  $2\% \pm 5\%$  Si and  $4\% \pm 6\%$  Ca, with  $20\% \pm 20\%$  OC.<sup>71,72</sup> The global composition of NPs in aquatic systems strongly resembles the distribution obtained from soils from which they originate.

Inorganic NPs are frequently coated by OM of terrestrial origin (e.g. HS), or exist as (OM)-hetero-aggregates (nano-assemblages) created by association with biogenic OM (e.g. biopolymers or proteins), where both types of OM form “eco-coronas” around NNP.<sup>73</sup> Analogous with ENPs, this natural organic capping is responsible for the stability of NNP and governs their fate in aquatic systems, and thus their variable composition and behaviour merit systematic study.<sup>74</sup> Humic organic materials and protein-based or protein-like macromolecules in aquatic systems can be separated by AF4 and distinguished with detectors such as fluorescence.<sup>75,76</sup> More accurate quantification of the elemental composition of larger NNP hetero-aggregates was achieved for NPS isolated from a highly productive lake using AF4-ICP-MS by optimizing their isolation and preservation (filtration membrane pore size), and their introduction into the ICP-MS.<sup>77</sup> However, others argue that extracting and/or stabilizing NNP offer a more promising

approach for improving their identification and quantification.<sup>78,79</sup> The effect of NNP extraction/stabilization on the size distribution and speciation of TEs associated within NPS requires additional study to explore their naturally occurring transfer, mobility, and potential toxicity.

**2.2.2. Size-based distribution of TEs.** The capacity of AF4 to decipher the preferential association of TEs within the size distribution of NPS was recently reviewed.<sup>80,81</sup> By increasing the retention of NPs to  $>300\text{ Da}$ , the *in silico* signal deconvolution of small oxides from humic-associated TEs also makes it possible to quantify these TE associations for both NPs  $< 25\text{ nm}$  and larger colloidal assemblages.<sup>6</sup> This is illustrated in Fig. 3D, where similar terminology to Fig. 1 can be applied. This type of differential association of TEs with HS and small oxide NPs is representative of boreal, sub-arctic water systems with abundant wetlands, which provide DOM and changes in redox conditions, or forested environments impacted by large terrestrial inputs of Fe, Mn, and/or Al with stabilizing organic matter. In these environments, changes in the agglomeration state of HS and/or associated TEs occurring during their dispersion were revealed at the confluence of both rivers and a river and lake.<sup>61,67</sup>

The pH-, HS content-, and iron loading-controlled colloidal As in a stream watershed was characterized using AF4-ICP-MS, together with its overall distribution amongst various types of NPs and simpler complexes in the dissolved phase.<sup>82</sup> The use of AF4-ICP-MS has also highlighted the competition between P and As at the surface of iron oxides in streams with similar characteristics.<sup>83</sup> This phenomenon may explain the discrepancies in As transport predictions, highlighting the need to incorporate nanoparticle dynamics in reactive transport models. Measuring these dynamics using AF4-ICP-MS and spICP-(TOF)MS for comparison with and improving these models remains unexplored.

The change in the proportion of small iron oxides and its effect on the seasonal dispersion of U associated with colloids were also quantified in the waters of a pristine wetland using AF4-ICP-MS.<sup>47</sup> As highlighted in Fig. 3A, oxygenation of naturally anoxic wetland water led to the formation of HS + Fe-containing NPs with oxidized U absorbed on the surface or occluded within nanoparticles together with OM, and the association of U with small HS.<sup>47</sup> Thus, the adsorption of U on NPs was shown to depend on the HS content, together with the pH. AF4-ICP-MS was previously found to be an ideal tool for quantifying the adsorption of uranium on synthetic hematite, with a decrease in its loading for small variations in pH (Fig. 3B, pH 4.2 and 3.6).<sup>84</sup> Using multi-angle light scattering (MALS), the major NPs carrying natural U were shown to be rod-like Al//Fe/C particles.<sup>85</sup> However, NPs carrying anthropogenic U from contaminated ponds mixed with groundwater were predominantly spherical and contained higher levels of iron. These examples demonstrate the ability of AF4-ICP-MS to quantify the changes in NP composition and shape related to their generation mechanisms and origin, and their distinct roles in TE dispersion.



The contribution of NPs to groundwater chemistry has received particular attention in recent years, in both natural and anthropogenic contexts.<sup>66,86,87</sup> The confluence of anoxic and surface waters was found to have a major influence on the size-based distribution of TEs, and served as a considerable source of NNPs.<sup>82,86</sup> Groundwaters beneath dredged sediment disposal facilities contained elevated levels of rare earth elements (REEs) with diverse NP populations.<sup>66</sup> These elements were often associated with Al and/or HS, but not systematically, suggesting distinct geochemical forms dependent on groundwater chemistry elucidated using AF4-ICP-MS (Fig. 3C). In contaminated sites of the Jiangxi Province (China), a switch from inorganic colloids to organic-rich colloids (HS) as the primary forms assisted the dispersion of REEs in groundwaters. This latter phenomenon was especially observed for high atomic mass REEs.<sup>87</sup>

In addition to being complexed by HS as chelates, adsorbed on the surface of NP, or coprecipitated within small oxyhydroxides of different crystallinity, shapes, and sizes, some TEs were naturally occluded in stable mineral structures originating from the weathering of rocks and other anthropogenic or natural processes.<sup>88,89</sup> Given that AF4-ICP-MS allows multielement detection, the quantification and proportions of elements contained in NPs can be used to identify the sources and geological origin of NNPs and NPs. In the particular case of REEs, the use of shale-normalized patterns and anomalies can distinguish anthropogenic and natural sources; this analysis should be applied to AF4-ICP-MS to investigate the size-resolved REE distributions in NPs. The combination of REEs and other elements can also be used to identify the origin of their nanoforms, as reported for Ce- or Ti-containing NPs.<sup>79,90,91</sup>

### 2.2.3. Complementarity of AF4-ICP-MS with spICP-MS.

Preconcentration can improve the detection of NPs and their associated TEs in water systems containing low NP counts and TE loadings by AF4-ICP-MS.<sup>92–94</sup> However, combining AF4-ICP-MS with spICP-MS, with much lower particle number detection limits is an advantage. To date, studies are still limited on the characterization of NNPs present in natural aquatic systems, but most illustrate the feasibility of measuring and potentially tracing inputs of ENPs, considered as trace contaminants.

Progress in the analysis of aquatic systems by spICP-MS is also oriented towards developing extraction methods<sup>95</sup> and decreasing the ionic background.<sup>96</sup> Although it is not a natural NPs, an ion-exchange resin was applied to remove the ionic background of samples collected from wastewater treatment plants (WWTPs), improving the limit of detection. Consequently, lower masses of Ca, Co, Au, Fe, Mg, Mn, Ni, and Zn could be measured using quadrupole sp-ICP-MS.<sup>97</sup> Combining an in-line ion-exchange resin to remove the ionic background of Zn with ultra-sensitive sector-field spICP-MS has also facilitated the detection of particles with an equivalent size detection limit as low as 14.3 nm in river waters.<sup>98</sup> To account for the ionic background and matrix effects, the use of calibration standards prepared in ultra-

filtered water (<1 kDa) from the original site of sampling was a good strategy for determining the background equivalent diameter for CeO<sub>2</sub>- and TiO<sub>2</sub>-containing NPs naturally occurring in the Seine River and its tributaries measured using sector-field sp-ICP-MS.<sup>99</sup>

Large-scale studies were also recently conducted using spICP-MS, such as measuring the sources and dispersion of Pb- and TiO<sub>2</sub>-containing NPs across 66 sites, demonstrating the maturity of this method.<sup>100</sup> WWTP effluents, river waters, and an estuarine transect were analyzed with in-line dilution using an ICP-MS/MS system to reduce interferences and high salt/carbon loading from the seawater. MS/MS was used in mass-shift mode to resolve interferences for Ti. The mass detection limit for particulate Pb varied from 0.8 to 5.7 attograms, and the equivalent size detection limit of TiO<sub>2</sub>-containing particles ranged from 24.4 to 72.5 nm depending on the ionic background. In some cases, Pb was adsorbed on the surface of particles more than occluded inside, illustrating that spICP-MS can also distinguish metal exchange on the surface of particles.

Both AF4-ICP-MS and spICP-MS were applied to measure the size distribution of Ag- and TiO<sub>2</sub>-containing NPs entering, passing through and exiting four WWTPs.<sup>90</sup> The source of the Ti-containing NPs was determined using AF4-ICP-MS to measure the Ti/Nb ratio of size-fractionated NPs. Only influent water was analyzed due to the limited number of particles in the effluents, using a 20-fold pre-concentration with an ultrafiltration device.

An spICP-MS methodology was also established for the long-term monitoring of Ag- and TiO<sub>2</sub>-containing NPs in diverse aquatic systems, addressing the urgent need for field measurements to validate and improve material flow analysis models.<sup>62,101</sup> Monthly sampling was conducted over one year in three small creeks with different land uses within the Seine River watershed in France (forested, agricultural, and urban) to investigate their temporal and spatial variations. The Ag-containing NP concentration ranged from  $1.5 \times 10^7$  to  $2.3 \times 10^9$  particles per L and 0.4 to 28.3 ng L<sup>-1</sup>. Different factors influenced the stability of the Ag-containing NPs in each watershed, where NOM controlled the Ag-containing NP behavior in the forested watershed, and major cations such as Ca influenced the Ag-containing NPs in the agricultural and urban watersheds. The specific higher export rate in developed areas suggested the constant release of Ag-containing NPs from consumer products. The average TiO<sub>2</sub>-containing NP concentrations were  $1.1 \times 10^9$  particles per L and 3.7  $\mu\text{g L}^{-1}$  across all sites, and seasonal variations were observed in forested and agricultural catchments. The highest land-area normalized annual flux of  $1.65 \text{ kg TiO}_2 \text{ year}^{-1} \text{ km}^{-2}$  was found in the agricultural catchment later, while the positive correlations between TiO<sub>2</sub>-containing NPs and trace elements/DOC in forested and agricultural catchments suggested geogenic origins. This study provides the first comprehensive dataset for Ag- and TiO<sub>2</sub>-containing NP fluxes in French surface waters over an extended period, demonstrating the influence of time, land use, and aquatic geochemistry.



Parallel to this study,<sup>101</sup> an AF4 system coupled online to UV, differential refractive index (DRI), MALS and quadrupole ICP-MS detectors was employed for the characterization of Ti-containing NPs in the three watersheds (Fig. 4), where the NP number concentration was a limiting factor for UV, DRI and MALS detection, and used to determine the absolute size of the particles. An in-channel pre-concentration method (large volume injection) was developed using a stabilized standard suspension of engineered  $\text{TiO}_2$ -NPs (see ESI,<sup>†</sup> section S3), allowing quantification at natural concentrations, 10 to 500 times lower than the original configuration. The fractograms obtained for the 3 natural samples showed the co-elution of

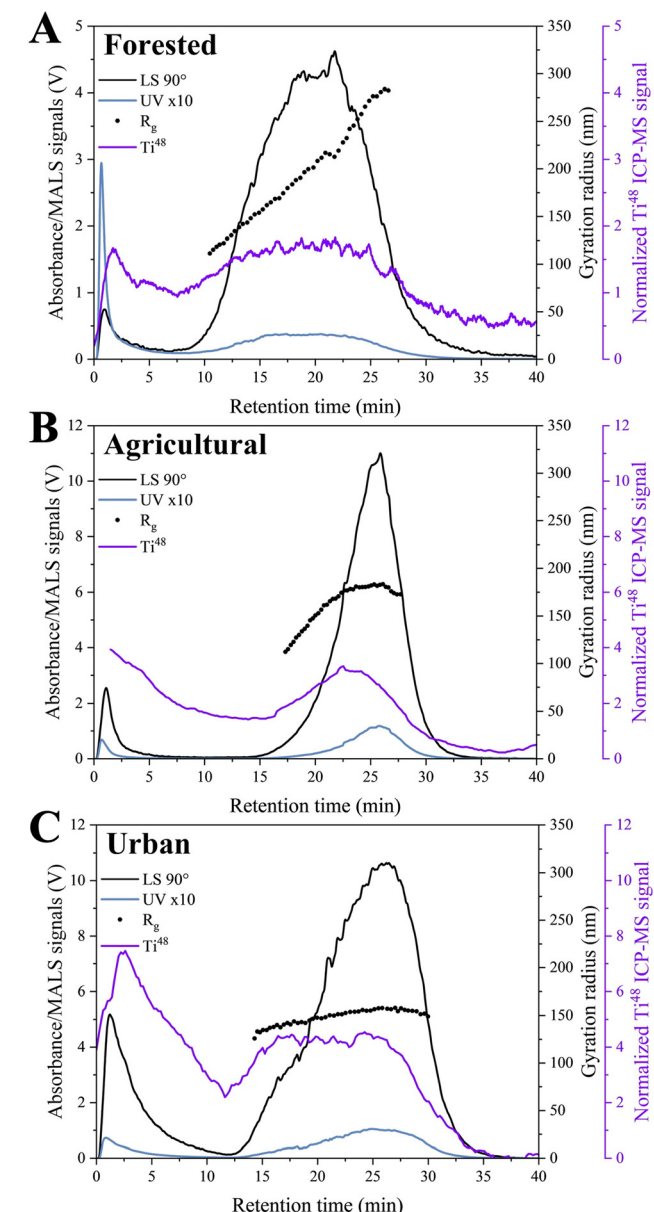


**Fig. 4** Characterization of NPs contained in river waters from A) forested, B) agricultural and C) small urban watersheds by AF4 in-channel pre-concentration and UV-MALS-ICP-MS. Fractionation conditions and settings are provided in ESI,<sup>†</sup> section S3 (unpublished data).

**Table 1** Size characterization of NPs in river waters from forested, agricultural and small urban watersheds obtained using MALS: number average ( $R_n$ ), weight average ( $R_w$ ), z-average ( $R_z$ ) and median radius of gyration ( $R_g$ ) in nanometers. The uncertainties come from the model used to fit MALS data

Site	$R_n$	$R_w$	$R_z$	Median $R_g$
Forested	$158 \pm 3$	$198 \pm 4$	$228 \pm 4$	191
Agricultural	$150 \pm 4$	$170 \pm 6$	$177 \pm 7$	177
Urban	$148 \pm 8$	$151 \pm 8$	$153 \pm 9$	153

ICP-MS and UV signals, qualitatively demonstrating that the signals corresponded with NPs that contained Ti (Fig. 4). A slightly larger size distribution was measured in the forested sample, while urban river water showed a lower average and median radius of gyration. Assuming that the Ti detected in the NPs was present as  $\text{TiO}_2$ , the equivalent spherical diameters obtained by spICP-MS ranged from 60–120 nm, 2 times smaller than the values reported for AF4-MALS (Table 1).

On one hand, questions remain about potential agglomeration during in-channel pre-concentration and memory effects in the AF4 injection loop; on the other hand, the data treatment and assumption of sphericity in spICP-MS analysis may underestimate the particle size. Two further factors should be considered, *i.e.*, size fractionation can occur during the nebulization step, sending larger particles to the drain *via* the spray chamber, and the ionization efficiency of a single  $\text{TiO}_2$ -containing NP also would not be the same as a hetero-aggregate. Moreover, the diameters evaluated by MALS measure the entire NP, which may be a composite of multiple elements including the carbon eco-corona, whereas spICP-MS only measures the equivalent  $\text{TiO}_2$  core size.

To compare the results of these methods, the spICP-(TOF)MS and AF4-ICP-MS communities should establish a consensus on sample and data treatment and adopt standardized protocols for the collection, storage, and analysis of samples to improve the intercomparison across studies and complementary techniques. Alternatively, this study confirmed that in-channel pre-concentration for AF4 merits further consideration. This opens the door to the characterization of NPs (including NNPs, INPs or ENPs) in samples limited by low NP loading, which is a current limitation of AF4-ICP-MS in comparison with spICP-(TOF)MS.

**2.2.4. Further considerations for spICP-TOFMS.** Although it has higher mass detection limits (size-equivalent diameters), spICP-TOFMS shows promise for the complete characterization of the NPs TE composition. It allows the measurement of isotopic and elemental ratios at the level of individual particles, which can be directly related to their source (natural background *vs.* ENPs), for which it was primarily developed and applied.<sup>57,79,102</sup> This method has recently been shown to be a versatile and robust approach for differentiating Ti-containing ENPs from Ti-containing NNPs.<sup>11</sup>

Interestingly, spICP-TOFMS was successfully employed to characterize the composition/origin of NNPs and colloids of  $<1.2 \mu\text{m}$  from the Seine River, and to study the effects of

filtration and centrifugation on their abundance and characteristics.<sup>60</sup> The potential presence of small oxides associated with larger calcite particles was also suggested, highlighting the value of spICP-TOFMS for identifying new mineral structures.

Only one example has illustrated the complementarity of measurements achieved by combining AF4-UV-ICP-MS and spICP-TOFMS in a boreal aquatic system.<sup>7</sup> As illustrated in Fig. 3D, the size distribution of Pb differed according to the river and with hydrological changes, which was related to the presence and stability of Fe and Mn oxides. Larger-sized particles measured by spICP-TOFMS corroborated this finding. This study also revealed that the composition and size of the smaller size range of NPS measured by AF4-ICP-MS did not vary in the same way as the larger equivalent size range of NPS measured by spICP-TOFMS both in various rivers and as flow rates change, suggesting different sources and mechanisms of NNPs generated from various populations or processes.

This in-depth characterization of NPS and their underlying populations of NNPs must be extended to other types of aquatic environments to better assess the range of both NNPs and NPS, considering the constraints imposed by low concentrations in certain systems. Recent applications show the capacity to pre-concentrate NPS for AF4 analysis and to decrease the size limit of detection for spICP-MS by using instruments dedicated to single-particle analysis. This opens avenues for future work in environmental nanobiogeochemistry by combining these techniques to analyze and compare the range of NPS and their underlying NNP populations across the complete size continuum in challenging aquatic environments.

### 2.3. Biological systems

As reported in previous sections, AF4-ICP-MS and spICP-(TOF) MS have demonstrated their value for the size-based distribution of elements, which have reached thermodynamic equilibrium, and for dynamic processes such as NNP generation. Biological systems are also better described with short-term dynamics, where metal exchange or eco-corona formation can occur, rather than the equilibrium state, with consequences for measuring the aggregation of NNPs and colloids. All these processes are well-recognized to mitigate the toxicity of metal species and often associated with a range of different organic components, as reviewed recently.<sup>103,104</sup> However, the implication of these simultaneously occurring processes under environmentally relevant conditions in the context of NPS remains to be explored. Despite the paucity of applications of AF4-ICP-MS for studying the interaction of NPS with biological systems, the capacity of this integrated technique for unraveling these bioprocesses has been demonstrated. For example, a bacterial siderophore was shown *in vitro* to selectively mobilize iron, but not Zn or Cu from humic substances isolated from several surface waters.<sup>105</sup> More recently, metal substitutions at potential targets of toxicity and scavengers in cells such as protein or peptide binding sites were

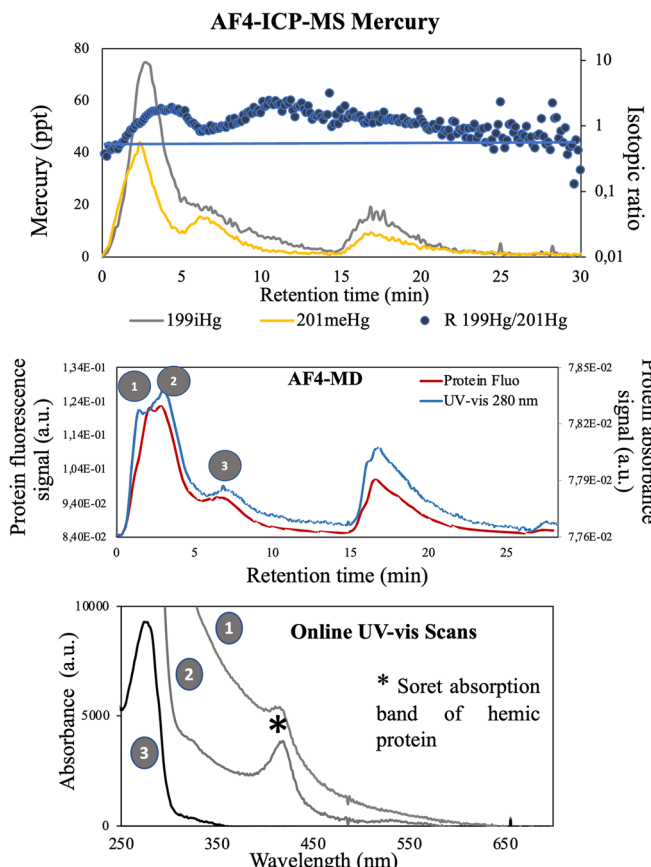
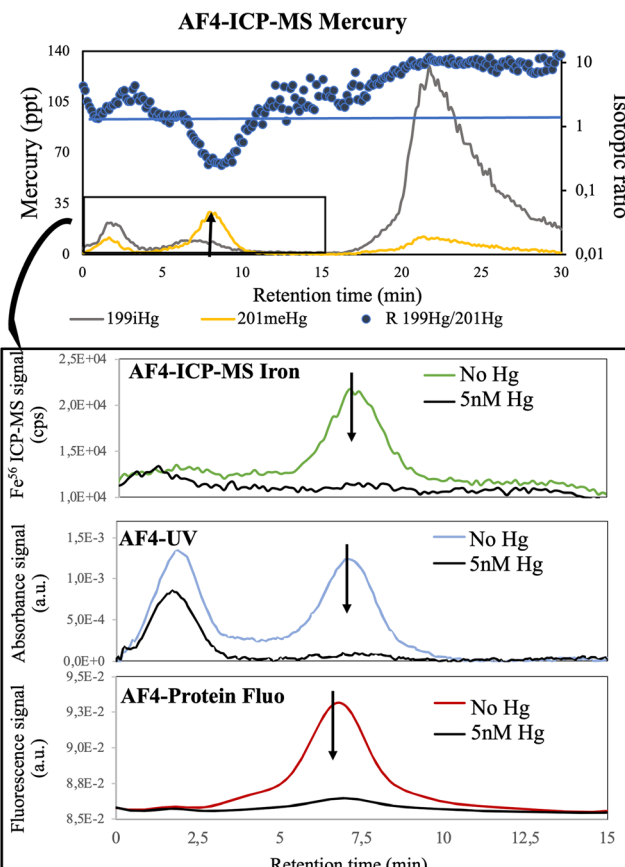
also quantitatively related *in vitro*.<sup>106,107</sup> The capability of AF4-ICP-MS to probe the effect of small bio-ligands on the stability of ENPs by eco-corona formation, followed by assisted dissolution was also recently demonstrated.<sup>108</sup> Notably, the state of ENP aggregation may alter their toxicological effects for microorganisms, while protecting the human hepatocarcinoma HepG2 cell line, as demonstrated for a safer-by-design biocide.<sup>109</sup>

From an ecotoxicological perspective, it is also important to highlight that organisms, regardless of their genus, influence the speciation of TEs through feedback mechanisms, which are often overlooked in ecotoxicological tests.<sup>110</sup> In this context, the interaction between metal species and autochthonous organic matter synthesized *in situ* by living organisms (secretome) as opposed to pedogenic matter (humic substances) or individual bioligands still requires a deeper mechanistic understanding. These interactions have been examined in recent reviews for Hg (ref. 111) and ENPs.<sup>112–114</sup>

Fig. 5 illustrates the characterization of Hg interactions with extracellular polymeric substances (EPS) released by phytoplankton using AF4-UV-Fluo-ICP-MS (Fluo: online fluorescence detector). The characteristics of EPS produced by two phytoplankton species differed, where EPS released by the diatom *Cyclotella meneghiniana* contained proteins with a molecular mass (MM) ranging from 35 to 165 kDa,<sup>114</sup> while the EPS produced by *Synechocystis* sp. were characterized by large hetero-aggregates with sizes up to 200 nm, composed of Fe, phosphate, and proteins.<sup>81</sup> Following a double isotope spiking procedure, the simultaneous size-preferential association of inorganic (<sup>199</sup>iHg) and methyl mercury (<sup>201</sup>MeHg) to EPS components released by the phytoplankton species was revealed using quadrupole AF4-ICP-MS. Using the isotopic ratio, the association of iHg and MeHg to diatom EPS was shown to be equivalent over the size continuum, with values varying as  $R_{iHg/MeHg} \sim 3$  (Fig. 5A). Additionally, the results identified an Fe-binding protein characterized by a hemic cofactor (Soret absorption band) in the EPS of *C. meneghiniana*. Based on its UV-visible spectrum, this property was not affected by the addition of Hg, despite both iHg and MeHg coeluting with the hemic protein (Fig. 5A). Contrarily, the fraction of protein that preferentially bound iHg was apparent in the larger entities for EPS released from cyanobacteria ( $R_{Hg/MeHg} > 10$ ), while MeHg was enriched in the low molecular mass components (Fig. 5B). The latter entity was characterized as a small Fe-containing protein produced by *Synechocystis* sp. (MM 30 kDa) using AF4-Fluo-ICP-MS, specifically interacting with MeHg but not iHg ( $R_{Hg/MeHg} \sim 0.1$ ). This interaction resulted in the displacement of the Fe content and quenched its absorbance and fluorescence (arrows in Fig. 5B). The latter result suggested the presence of a potential target for MeHg in the EPS of *Synechocystis*.

Overall, this example highlights the otherwise relatively unexplored capacity of AF4-UV-Fluo-ICP-MS to characterize macromolecules present in complex and heterogeneous mixtures and identify their role as potential targets of metal binding, which can be connected to detrimental effects or



**A. Cyclotella EPS + iHg/MeHg****B. Synechocystis EPS + iHg/MeHg**

**Fig. 5** Size-resolved analysis of simultaneous mercury ( $^{199}\text{iHg}$ ) and methyl-mercury ( $^{201}\text{MeHg}$ ) interactions with EPS components released by a diatom, *C. meneghiniana*, (A) and a cyanobacterium, *Synechocystis* sp., (B) using AF4-ICP-MS and UV-Fluo. The isotopic ratio is present as the log of  $^{199}\text{iHg}/^{201}\text{MeHg}$ . The ratio increased as iHg bound to EPS increased compared with MeHg ( $>1$ ), but decreased when MeHg bound to EPS increased compared with iHg ( $<1$ ). The UV-vis scans, obtained at different retention times with AF4-MD (labelled 1, 2 and 3) are presented, allowing the identification of hemic protein with Soret absorption band (\*) eluting mainly at retention time 2. Fractionation conditions and settings are provided in ESI;† section S4 (unpublished data).

protection against toxicants. Thus, AF4 provides an in-depth assessment of the dynamics of metal species transformations at the macromolecular/nano size-continuum.

Due to potential co-elution of different metal species in AF4 based on their similar hydrodynamic diameters, the presence of neo-mineralized elements in complex biological matrices cannot be conclusively demonstrated solely using this technique. Alternatively, spICP-MS can function as a complementary technique to address this limitation. A recent study illustrated the use of spICP-MS for refining the toxicity of Cr based on its speciation, given that under normal exposure conditions this element forms NPs, resulting in the inappropriate evaluation of the EC50 for aquatic organisms.<sup>115</sup> The capacity of living organisms to synthesize *de novo* nanoparticles from ionic exposure as depuration mechanisms was also recently highlighted *via* the spICP-MS analysis of a diatom exposed to ionic Hg.<sup>116</sup> The formation of HgSe-containing NP as a common detoxification pathway for Hg was also demonstrated using spICP-(TOF)MS in bird organs (liver, kidneys, brain, and muscles)<sup>117</sup> and a cetacean.<sup>118</sup> In the latter study, AF4-MALS-ICP-MS/MS and spICP-TOFMS were used to

address the size distribution of metal nanocomponents extracted from the liver and cerebellum of a sperm whale, highlighting the bio-corona surrounding the newly formed HgSe- and Cd-containing particles. Combined, these studies demonstrate the potential, accuracy, and versatility of spICP-MS for analyzing environmental NPs in biological samples, and the use of AF4 and spICP-MS together to compensate for their limitations.

Processes involving OM interactions with NPs such as bio-corona transformation and OM-NP hetero-aggregation can also be identified, characterized, and quantified using AF4-ICP-MS.<sup>106,107</sup> In the case of Ag-NPs and *C. meneghiniana* EPS, eco-corona formation involved mainly proteins, and also exopolysaccharides, hindering the strong aggregation forces induced by high ionic strength.<sup>114</sup> This co-occurred with the formation of smaller and polydisperse hetero-aggregates bridged by EPS. The high versatility and combination of AF4 with Fluo, UV and ICP-MS detectors also measured the formation of a protein corona from diatom *C. meneghiniana* EPS around Ag-NPs.<sup>114</sup> Further, AF4-UV-ICP-MS provided important information regarding the aggregation state of the



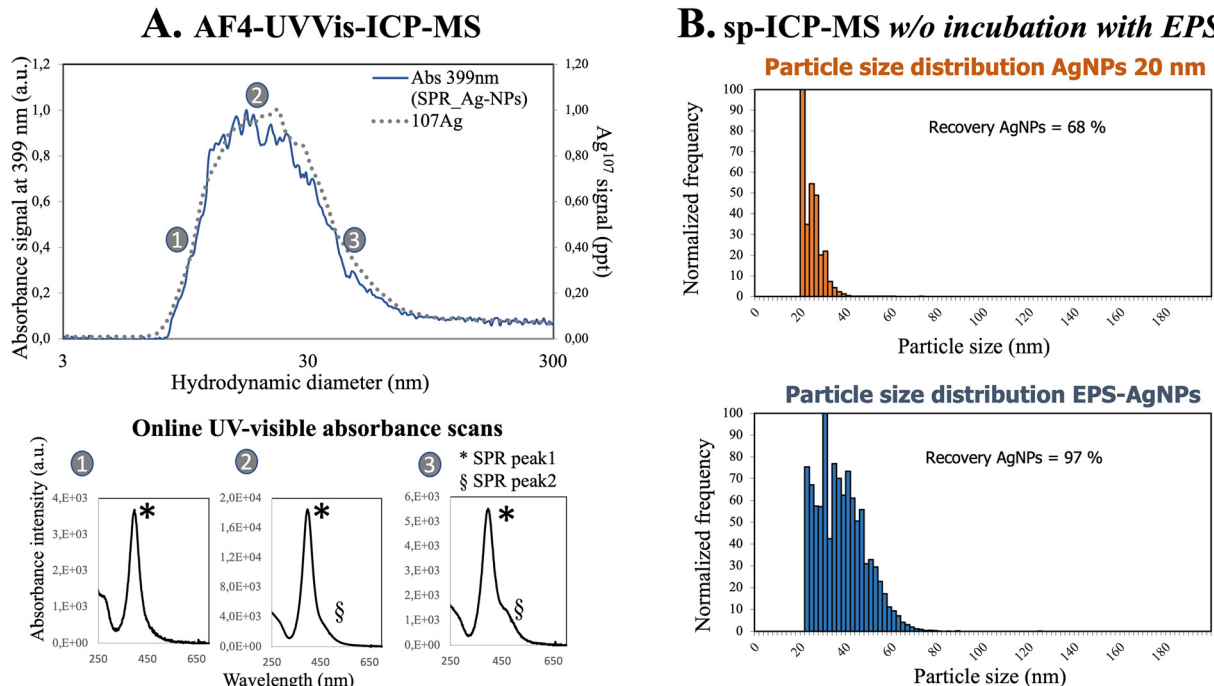


**Fig. 6** Complementarity of A) AF4-UVVis-ICP-MS and B) sp-ICP-MS for the characterization of Ag-NP hetero-aggregates formed in the presence of *C. meneghiniana* EPS. Absorbance of Ag-NP and Ag signal coelution in AF4 were related to online UV-visible scans extracted from diode array detector data at (1) the beginning, (2) maximum and (3) end of the size distribution. Ag-NPs were characterized by the presence of a surface plasmon resonance band (SPR, peak 1) with a maximum absorption wavelength of 392 nm and presented a second SPR band (peak 2) upon hetero-aggregation. The equivalent particle size distribution and proportion of nanoparticulate Ag (recovery nAg) quantified using sp-ICP-MS for Ag-NP hetero-aggregates (blue) were compared with that obtained for the original Ag-NP suspension (orange). Fractionation conditions and settings are provided in ESI;† section S5 (unpublished data).

Ag-NPs, using their surface plasmon resonance (SPR) signatures collected over their complete size distribution (Fig. 6A; the online UV-visible scans indicate that aggregation increased with retention time). The  $d_h$  of Ag-NP hetero-aggregates measured using AF4 with external calibration underestimated their size ( $d_h = 17$  nm) compared with the equivalent diameter determined using sp-ICP-MS ( $d = 25$  nm).<sup>119</sup> The aggregation of Ag-NPs induced by *C. meneghiniana* EPS was confirmed by sp-ICP-MS (Fig. 6B), showing the advantage of working at more environmentally relevant concentrations compared to the online UV-visible scan measurements. However, the equivalent size detection limit of the ICP-MS instrument used herein was above  $d = 20$  nm, leading to a truncated size-distribution for the original engineered Ag-NP suspension (20 nm, with an estimated nanoparticulate recovery (nAg) of 68%) (Fig. 6B). The size distribution of Ag-NPs became wider in the presence of EPS and shifted towards larger particle sizes, with the nAg recovery increasing to 98%. The larger quantity and particle size of nAg obtained after 24 h of incubation suggest the (hetero)-aggregation of Ag-NPs and the hindrance of their dissolution by EPS.<sup>114</sup>

Finally, single-particle analysis is not only constrained to the measurement of nano-objects or their assemblies but can be applied for the quantitative determination of the elements present in cells. The applications reported for the analysis of

unicellular organisms by single-cell (sc)ICP-MS in biomedical and environmental research were recently reviewed.<sup>120</sup> By increasing the transfer of cells into the ICP,<sup>121</sup> the form of intrinsic elements that are essential or toxic as hydrated ions or NPs and their uptake into or association with cells can be measured.<sup>122</sup> Single-cell analysis is also considered to better represent the biological diversity in metal species uptake compared to bulk analysis (after digestion/mineralization of cells). For instance, the bio-uptake and strong sorption of both dissolved Au and Au-NPs in the freshwater alga *Cryptomonas ovata* and their distribution in individual cells were measured using scICP-MS, demonstrating that only 40–50% of the cells contained NPs.<sup>123</sup> Understanding the cell-to-cell variation in the metallome composition provides in-depth information about the essential role of trace metals in signaling, catalysis and gene expression, and the structural integrity of DNA and RNA, among other biological functions that can be disrupted by exposure to toxicants. Because cell introduction can lead to interference in the  $m/z$  in ICP-MS, the use of higher resolution mass analyzers is required to avoid misleading conclusions. Thus, the potent resolution of ICP-MS/MS was used to determine the distribution of P in bacterial cells using mass-shift mode and a reaction cell with  $O_2$ , using  $^{31}P^{16}O^+$  as the target ion.<sup>124</sup> Moreover, in another study, the P, S, Mg, Zn, and Fe contents of phytoplanktonic cells were also quantified using mass-shift mode ( $^{31}P^{16}O^+$



and  $^{32}\text{S}^{16}\text{O}^+$ ). On-mass mode with hydrogen reaction gas was used to measure other challenging elements such Mg, Zn and Fe.<sup>125</sup> The growth of magnetite and the corresponding proportion of ionic Fe that was internally mineralized by magnetotactic bacteria were quantified by sector-field scICP-MS.<sup>126</sup> A recent study also quantified the simultaneous uptake kinetics of Hg- and MeHg-enriched isotopes by unicellular algae using scICP-MS and scICP-TOFMS, and addressed the changes in the population-level metallome of algae exposed to the latter.<sup>127</sup> The possibility of accessing the metallome composition at the single-cell level using scICP-(TOF)MS opens new opportunities for distinguishing cells/microorganisms from non-living organic materials. This allows the quantitative assessment of the interactions between microplastics and living cells, using either metallic labels or intrinsic carbon signals.<sup>128,129</sup>

Relating the processes involved in the bio-interactions of metal-species present at the nanometer and macromolecular scales, at doses relevant to their uptake, at the level of single cells, constitutes the first step towards understanding toxicological events. Thus, combining AF4-ICP-MS with spICP-MS and scICP-MS enables the quantification of bioprocesses occurring at trace doses and small size-scales, with the minimum time required for sample preparation and analysis compared to other techniques. Taking advantage of the in-depth size-resolved characterization of NPs and their associated elements by AF4-ICP-MS and sp/scICP(TOF)MS will provide insights into their global bioprocessing in the environment, and more realistic knowledge of their ecotoxicological impact.

#### 2.4. Recent progress in economic geology

Although economic geology is not typically considered a component of environmental chemistry, they are closely linked through their study of the transport and elemental associations of metals in natural systems. Furthermore, many of the same biogeochemical processes discussed above are highly relevant to mineral deposit formation and exploration and assessing the environmental impacts of mining activities. Thus, the recent application of nano-analytical methods in this field is briefly considered below.

Because natural nanomaterials are abundant in all environmental compartments, they play key roles in the cycling of both rock-forming and trace-level elements throughout earth systems. Significant areas of research include mineral weathering and dissolution, metal transport and deposition in the context of mineral deposits, and mineral-microbe interactions.<sup>130-132</sup> However, the low throughput of microscopy techniques is a persistent challenge in these nanogeoscience studies. Millions to billions of NPs can be suspended from one gram of soil or sediment, requiring high throughput techniques for their effective characterization.

Recently, AF4-ICP-MS and spICP-MS have been used in nanogeoscience, focusing on the mineralogy and elemental associations of NNPs. The goals of this work have been to better

understand their cycling in geological systems, and their relevance to broader geoscience applications such as economic geology. The AF4-ICP-MS system has been proven to be effective for determining the size-resolved distribution of trace elements, including REEs in acidic groundwaters, which were investigated as a secondary source of critical minerals.<sup>66</sup> In this unique environment, AF4-ICP-MS provided key insights about the particulate fractions of REEs that would otherwise be classified as “dissolved”, following the operational definition of passing through a 0.45  $\mu\text{m}$  filter. Distinct nanoparticulate phases of REEs are shown in Fig. 3C, including those likely bound to organic matter, those associated with Al (indicating adsorption to clays or hydroxide minerals), and a unique class of intrinsic REE-containing NPs. The identification of REE-containing NPs has implications for the recovery of REEs from secondary sources; different processes are required for aquo complexes *vs.* adsorbed REE species *vs.* REE mineral NPs. Although AF4-ICP-MS does not have the capability to characterize individual NPs, it will continue to find uses in economic geology. With the recent focus on the role of colloidal gold in forming high-grade Au deposits, the potential for AF4-ICP-MS to investigate Au-containing NPs in active hydrothermal systems can be inferred.<sup>133</sup>

As described above, spICP-MS has revolutionized the measurement of NPs in environmental systems due to its high-throughput capability. Because mineral NPs are orders of magnitude more abundant by number than larger mineral grains, spICP-MS has emerged as a new tool to aid studies across geoscience wherever large mineral grains are rare. Because “indicator” minerals are used to identify buried ore deposits, the use of spICP-MS to rapidly detect large numbers of mineral NPs has been suggested as a new method for mineral exploration. Gold- and Ag-containing NPs have been identified in stream sediments by spICP-MS to identify Au mineralization, with the potential for lower detection limits compared to conventional digestion procedures.<sup>134,135</sup> The multi-element capability of spICP-TOFMS has further characterized the nanoscale mineral diagnostics of pegmatite ore deposits, including Hf-rich zircon, and the rare minerals bismutotantalite and stibiotantalite.<sup>136</sup> The concentration and composition of Co-bearing NPs were also investigated in soil and regolith surrounding several types of cobalt deposits.<sup>137</sup> Co-NP associations with Mn, As, Fe, and Ti indicate possible mineral phases hosting Co, which can be used in future mineral exploration.

Studies of geochronology and provenance analysis rely on the analysis of isotope distributions in minerals such as zircon and monazite. Recently, spICP-TOFMS was used to investigate whether individual monazite NPs could be dated using Pb isotope distributions.<sup>138</sup> Although the precision was inadequate to allow meaningful interpretation of their age, this study offers insight into the future of nanogeoscience. Nano-scale minerals may be analyzed in rocks where minerals suitable for radiometric dating or provenance analysis are rare, with the advancement of the analytical capabilities of spICP-TOFMS. Recent studies have also demonstrated the use of a multi-



collector ICP-MS (MC-ICP-MS) to measure the isotopic and elemental distribution in NPs, increasing the precision compared to spICP-TOFMS by over an order of magnitude.<sup>139</sup> However, the faraday cup detectors used in MC-ICP-MS can only be operated at long (*e.g.* 50 ms) dwell times, which are inadequate for analyzing most natural samples. In the absence of a reliable method to date individual mineral NPs, spICP-TOFMS can instead be used as a screening tool to determine the abundance of these minerals, allowing the more targeted sampling of rocks to yield useful geochronological or provenance analysis. These are merely a few examples of areas where nanogeochemical analysis can aid investigations; in short, any study in geoscience that requires detection or characterization of an uncommon mineral is likely to greatly benefit from spICP-TOFMS analysis of more abundant nanominerals.

## 2.5. Recent advances in standardization

Stable and reproducible standards are necessary to ensure consistency between different experimental approaches and serve as a reference for comparative analysis of environmental samples to characterize TE behaviour and associated size fractions. Colloid standards and interlaboratory comparison can thereby help build the foundation for research in environmental nanogeochemistry, which seeks to measure and characterize the nature and functions of NPs and disturbances thereto, such as those caused by climate change or other anthropogenic disruptions. A large set of proteins and metalloproteins is available for both calibrating the size retention in AF4 (ref. 107 and 119) and quantifying some metals such as superoxide dismutase (Cu/Zn), hemoglobin, ferritin and myoglobin (Fe). However, they have a lower polydispersity in terms of size distribution and will not have the same type of membrane interactions and elemental compositions as NPs. More specifically, in aquatic ecosystems, TEs are present in multiple size fractions such as hydrated ions and other small, simple complexes, organic matter complexes, or larger primarily inorganic particles. Using AF4-UV-ICP-MS, the proportions of TEs associated with each size fraction may be examined, as exemplified above. The early steps toward the development of a mixed colloid standard with TEs adequately representing environmental samples for method standardization and comparisons using AF4-UV-ICP-MS across laboratories are presented below.

The primarily organic Fe peak represents a potential gradient of size and colloid type running from small OM-associated Fe ions, through OM-associated ferrihydrates and small Fe nanoclusters embedded in organic matter, through to larger nanoparticulate Fe with a substantial SRHA eco-corona. The presence/absence and relative amounts of the varying NP populations along this gradient require additional techniques such as TEM-EDXS for their assessment; however, the higher molecular mass of the OM-associated Fe/Pb peak (*ca.* 70 kDa) compared to the lower molecular mass of the OM and Cu-associated peaks (2–5 kDa) suggests that this Fe-dominated peak is primarily composed of Fe/Pb nanoclusters stabilized by the HA (Table 2). Given that Cu and Pb are added prior to Fe(II) oxidation, they become incorporated into OM and the amorphous Fe lattice structure due the high trace metal binding affinity exhibited by SRHA, Fe-SRHA complexes, and Fe oxyhydroxides with an SHRA eco-corona.<sup>140</sup> The similarities in peak shape, area and size for each component between repetitions indicated reproducibility of the standard synthesis and analysis (Fig. 7).

The molecular mass at the peak maximum of the fractograms (Table 2) and concentrations of metals associated with each peak (Table 3) were also determined. The similarities between the molecular mass of each component and Fe concentration values indicated the reproducibility of the results within batches. The same procedure can be applied for the Cu and Pb concentration determination in each peak (data not presented). This suggests the reproducibility of the preparation procedures, which can be further supported through interlaboratory comparison. Additionally, the concentrations in each peak relate to the peak sizes displayed in the fractograms. For example, a high Fe concentration was associated with the high peak intensity and area of the small DOM-associated components. The same relation for the smaller void and inorganic matter (large) peaks indicated that the dominant form of colloidal Fe was associated with organic matter in the form of complexes or small nanoparticle clusters. This was also true for Pb and Cu (data not shown), where the latter was mainly in the form of OM complexes.

The comparability of these results between and within batches suggests an effective standard for intra-laboratory comparisons. Further study can determine whether this standard is stable and the analysis reproducible over a sufficient time, or if changes in its synthesis are needed. Interlaboratory comparisons to determine stability and reproducibility across

**Table 2** Average molecular mass (kDa) for each analyte obtained for two sets of repetitions of the standards. Error bars show 95% confidence intervals assuming a Gaussian distribution

Component	Average molecular mass (kDa)			May 20 samples		
	March 15 samples		MR15 R3	May 20 samples		MY20 R3
	MR15 R2	MR15 R3		MY20 R1	MY20 R2	
OM	2.4 ± 0.2	2.36 ± 0.03		5.6 ± 0.1	5.6 ± 0.6	5.1 ± 0.1
Fe	62 ± 1	61.6 ± 0.7		68 ± 4	67 ± 4	66.7 ± 0.9
Cu	4.04 ± 0.07	4.3 ± 0.3		5.2 ± 0.4	4.8 ± 0.7	5.1 ± 0.8
Pb	75 ± 2	74 ± 5		67 ± 2	70 ± 4	66 ± 3



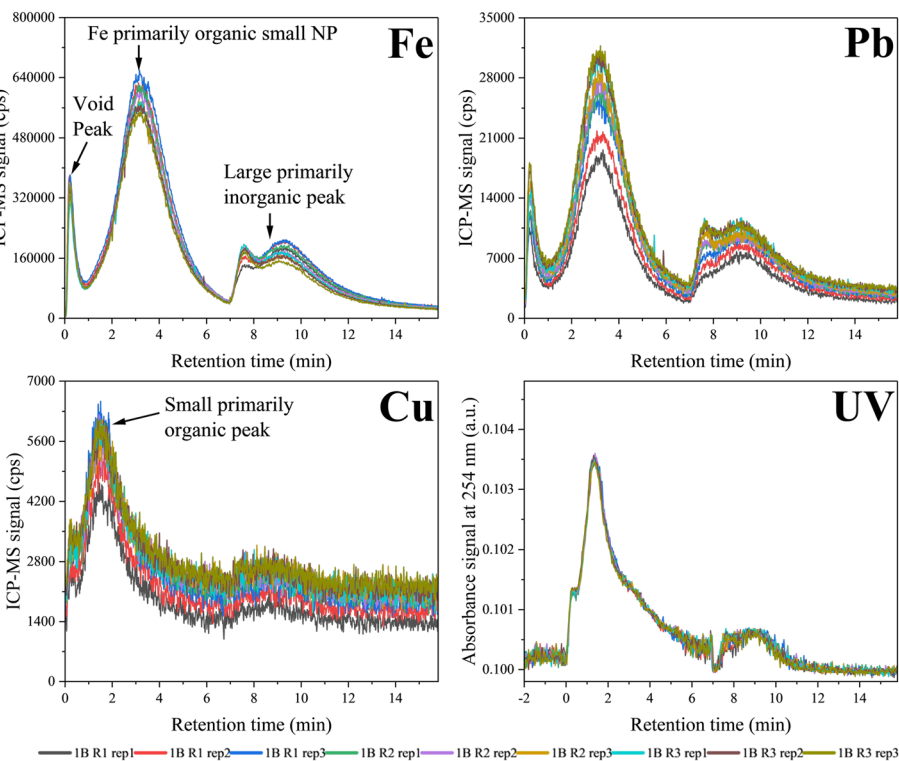


**Fig. 7** Fractograms for each component of three repetitions of the standard tested in triplicates obtained on May 20, 2024. Fractionation conditions, settings and experimental details are provided in ESI,† section S6 (unpublished data).

**Table 3** Average Fe concentration (ppb) in each peak for two sets of repetitions of the standard obtained in 2024

Peak	Average Fe concentration (ppb)			May 20 samples			
	May 7 samples	MY07 R1	MY07 R2	MY07 R3	MY20 R1	MY20 R2	MY20 R3
Void		23 ± 1	23.0 ± 0.8	24.7 ± 0.8	21.9 ± 0.4	21 ± 2	22 ± 2
OM associated		162 ± 4	170 ± 4	160 ± 6	189 ± 6	194 ± 9	195 ± 2
Inorganic		68 ± 2	94 ± 8	92 ± 4	79 ± 5	84 ± 4	81 ± 4

laboratories will indicate an effective colloidal standard for comparing results in future AF4-UV-ICP-MS research.

The choice of the selected components herein was motivated by the prevalence of Fe-OM nanoparticles in boreal rivers and forested watersheds, and their importance in the transport of trace metals and other potential contaminants. They can also be applied for the characterization of soil solutions or extracts, similarly rich in OM and Fe, as depicted in the previous section. In the case of natural systems with limited DOM and Fe redox processes, the composition of the standard can be modified to represent the system of interest. For example, this can involve changing the TEs or NNPs and organic material.

### 3. Frontiers and challenges

#### 3.1. Standardization of analysis and sample treatment

The systematic characterization of NPS and their deviations from natural conditions on a global scale requires analyses that

are reproducible or at least comparable across laboratories. ISO standards already exist for both AF4 (ISO/TS 21362) and spICP-MS (ISO/TS 19590), with comparison exercises aiming to characterize the particle standards recently proposed for both techniques. Furthermore, engineered NP standards with various sizes and elemental compositions allow the comparison and calibration of spICP-(TOF)MS across laboratories, and standards also exist to calibrate and compare AF4 flow programs based on molecular mass and size. Calibration standards, matrix-matched standard reference materials, and associated procedures for the calibration and comparison of ICP-MS across laboratories have been well established. However, these standards are not representative of the complex and dynamic mixtures of molecules, particles, hydrated ions, and simple complexes that comprise NPS. Thus, it is necessary to develop NPS standards containing mixtures of elements and particles similar to natural systems, such as NOM, NOM-coated inorganic nanovectors, and trace elements adsorbed to and occluded

within these ligands and particles. These mixed NPS standards are needed to compare methods within and across laboratories and to assess numerous potential artefacts associated with NPS, such as i) comparing and determining the detection limits for elements with low concentrations in individual multi-element particles in spICP-(TOF)MS;<sup>141–144</sup> ii) assessing and comparing potential artefacts associated with various AF4 separation conditions;<sup>80,145</sup> and iii) assessing the potential for aggregation, dispersion, dissolution, or other changes in speciation and size-based distribution during the storage and pre-treatment of NPS.<sup>31,60,146,147</sup> The systematic characterization of NPS and their deviations from natural conditions is ideally based on measurements that represent *in situ* conditions; however, this task can also be achieved if the deviation from *in situ* conditions is consistent and uniquely related to those conditions, enabling the state under the *in situ* conditions to be derived from the measured values. The range of current pretreatment and storage techniques in use includes storage under refrigerated conditions without treatment; freezing; filtration with 0.22, 0.45, or 1.2 µm filters; sonication to re-suspend and disperse particles and aggregates; cloud-point or solid-phase extraction to isolate particles for spICP-(TOF)MS; addition of a surfactant to disperse particles and aggregates; dilution to reduce the probability of overlapping particle signals in spICP-(TOF)MS; centrifugation as an alternative to filtration for isolating a particular size fraction, or to isolate the ionic background in spICP-(TOF)MS; and ultrafiltration for pre-concentration or to isolate the ionic background in spICP-(TOF)MS.<sup>7,62,96,146–148</sup> Given the impossibility of *in situ* measurements and requirement for pretreatment in AF4-ICP-MS and spICP-(TOF)MS, comprehensive assessments of the sample collection and storage impacts are needed to compare results across laboratories, and even within the same laboratory when the pretreatment or storage procedures differ.

### 3.2. Data analysis, fusion and integration

Advanced computational techniques are currently used to compare samples containing tens or hundreds of thousands of particles in each milliliter when analyzed by spICP-TOFMS, with up to 40 elements in each particle. Significant strides have also been made to identify the distribution and mass-dependent behavior of background events in spICP-(TOF)MS, allowing the calculation of a precise confidence level for confirming particle events.<sup>142</sup> However, the optimal method for detecting particles in the presence of a multi-elemental background of ions and small metal-containing molecules remains an active area of research. This is computationally challenging given that measuring 40 distinct masses in particles using spICP-TOFMS with a typical dwell time of 100 µs for a 2 min measurement yields nearly  $5 \times 10^6$  data points for a single sample.

Clustering and machine learning methods have also been applied to organize and identify natural nanoparticles according to type, respectively.<sup>8,11,51,57,60,149,150</sup> Environmental nanobiogeochemistry requires approaches that can identify

particle types within NPS that are related to their environmental functions, and types that are modified in number, size or composition in response to disturbances. This suggests the application of unsupervised methods such as clustering and self-organizing maps; however, some mapping between the known functionality of colloids with a known composition may also be useful. In some case, this mapping is achieved when AF4-ICP-MS is used to separate NPS into different forms of TEs that are associated with their hydrodynamic diameters, such as hydrated ions and other small, simple complexes, organic-associated, and primarily inorganic particles.<sup>6</sup> However, the relationships between the distribution of elements amongst these colloidal forms and the environmental relevance of NPS have received limited attention.<sup>28,151–153</sup> Conceptual and computational insights based on empirical data are also needed to optimally describe the nature and functionality of the complete NPS by integrating the distributions of smaller and organic-dominated constituents of NPS determined by AF4-ICP-MS with the particle-by-particle analysis of larger inorganic-dominated constituents determined by spICP-TOFMS.

Clustering and other machine learning procedures for classification also produce mathematical objects that may differ depending on the relative abundance of a wide range of nanominerals and mineral nanoparticles, in which case they are not likely to represent distributions or ratios of elements corresponding with singular minerals, but rather NPS-dependent groups of minerals. In this case, different NPS must be analyzed as part of a single clustering process for comparison, or new mathematical approaches are required to compare NPS across studies.

### 3.3. Characterizing the range of NPS, governing mechanisms/processes, and their dynamics

There are a staggering number of particles constituting the NPS in each mL of water in most natural aquatic systems, with similar potential for incredible heterogeneity. For example, it has been estimated that there are more than  $10^9$  particles per mL that are  $<120$  nm in the thermocline of the ocean, approximately 15 km offshore.<sup>154</sup> These may be primarily organic molecules, inorganic elements complexed by organic molecules, or any one of a range of forms of primarily inorganic oxides and oxyhydroxides of Al, Mn, or Fe with various amounts of organic material within their amorphous or crystalline structure, and on their surfaces.<sup>155,156</sup> Even if the properties and associated environmental relevance of each particle are determined, our ability to integrate these properties from the fine-grained scale of each particle is limited by the potential differences in the relevance of scale for various properties and functions, the non-additivity of interactions between particles, the dynamics of these interactions, and the lack of mathematical solutions to these multi-body problems.<sup>157–160</sup>

Thus, understanding NNP interactions and their combined roles in ecosystem functions differs markedly from that of bulk-phase impacts and typically homogenous groups of ENPs



because they are highly diverse, discrete entities that do not behave in an additive fashion. This divergence leads to inherently complex questions, such as how should the properties, interactions and impacts measured for individual NPs be mapped onto their nonadditive behaviour as NPs? Similarly, how should the diverse properties of NNPs in NPs be grouped or classified and combined or compared to connect them to interactions and impacts?

The description of NPs in terms of distributions amongst groups having known property-relevance relationships may serve as a sufficient approximation; however, this first requires the testing of these relationships for the environmental functions of interest. In the case of some environmental functions, reasonable approximations may also be found by employing tools and concepts from the fields of complex systems science, such as statistical mechanics, network theory, information theory, agent-based modeling, self-organization and self-organized criticality.<sup>161–166</sup> Machine and deep learning approaches may also be useful for uncovering property-relevance relationships and extracting key features to reduce the dimensionality in the calculation of multi-body interactions, and the associated emergent properties and functions of NPs.<sup>167,168</sup>

### 3.4. Connecting analyses to bio-/ecological consequences and global impacts

How the above-mentioned differences in metal association, mineral formation/form, and hetero-aggregate structures may influence the bioavailability of TEs that are associated with NPs to aquatic organisms represents a challenge for future research, together with determining how their size-resolved distribution may be modified following bio-interactions. To date, the effects of external conditions on the environmental effects of potentially toxic TEs under relevant environmental conditions (other than polluted systems) are unclear. This hinders our understanding of the key risks and issues associated with the detection of potentially toxic TEs according to their physico-chemical forms. The lack of information regarding the direct and indirect impacts of NNPs also makes it challenging to anticipate their consequences at the ecosystem level. Regarding the direct impact of NNPs on aquatic organisms, only limited studies have investigated their detrimental effects.

Recently, NNPs isolated from a river were found to be lyophilized dysregulated sub-lethal endpoints for the green algae *Chlorella vulgaris* (e.g. photosynthesis yield, amino acid metabolism, and reactive oxygen species production).<sup>169</sup> The potential effects of TEs contained in colloidal isolates (1 kDa–1.2 µm) induced toxic outcomes for the rotifer *Brachionus calyciflorus*, but not for the green alga *Pseudokirchneriella subcapitata*.<sup>170</sup> The biological endpoint chosen in the latter report was growth limitation, which is known to be the final toxicological state after organisms adapt to stress. However, as essential sources of nutrients, NPs can also promote the growth of certain species over others at the community level. For example, the reductive

dissolution of Fe-containing NPs released the P adsorbed on their surface, rendered it bioavailable for cyanobacteria in a lake, and responsible for their predominance at the bottom layer of the lake.<sup>171</sup>

Other species will take advantage of depuration mechanisms with consequences for the transformation of TEs and potential implications for higher trophic levels. For example, nano-HgS, which is the more stable form of Hg under anoxic conditions and considered non-available,<sup>172,173</sup> was transformed into methyl-mercury (neurotoxin) by a cohort of methylators, together with a part of the Hg(II) bound to particulate FeS and humic substances.<sup>174</sup> This suggests that the bioavailability of TEs and NPs need to be further explored in the context of NPs, especially changes in their speciation and size-based distribution at the bio-interface.

Given their larger diversity in both organic and inorganic compositions, the bio-impact of NNPs cannot be directly related to that of the largely explored ENPs, even when exposed in natural waters.<sup>175</sup> Thus, similar to ENPs and dissolved toxicants (including metals), addressing species sensitivity distributions for NPs isolated from different aquatic settings, including environments contaminated with TEs, will provide opportunities to address how and when NPs can lead to beneficial or detrimental effects on a particular ecosystem. Although environmental geochemistry applies a geochemical lens to the impacts of disturbances on natural systems at the bulk scale, their impacts on NPs have received little attention. Given their importance as potential sources, sinks, and transporters of contaminants and nutrients, more information is needed about the impacts of disturbances on the composition, properties, and ultimately environmental functionality of NPs.<sup>176</sup> Given the diversity of NPs and the natural processes that govern their composition and properties, in addition to the wide range of potential disturbances to governing factors such as hydrology, relative source fluxes, and variables controlling aggregation and sedimentation, significant effort is needed to measure the range of natural conditions within a system and deviations therefrom.

Understanding how disturbances may be coupled to positive and negative feedback loops is especially critical in the present era of global climate change, where NPs may play significant roles. For example, the climate-associated browning of boreal lakes and streams is associated with increasing exports of organic-coated Fe-containing NP, with elevated stability in conditions of increasing salinity.<sup>177–181</sup> Hence, this phenomenon will lead to the increased export of Fe to the oceans where it is a limiting nutrient for algae, potentially causing a net increase in carbon sequestration on the ocean floor. Quantifying the role of this NPs and others containing carbonate NPs that play important roles governing sources and sinks of carbon is needed to accurately quantify the impacts of increasing CO<sub>2</sub> levels and climate change and better characterize potential tipping points and feedback loops at the nanoscale.



### 3.5. Combined with additional tools/analyses

The use of AF4 and (sp)ICP-(TOF)MS for the separation and analysis of NPS provides the distribution of elements amongst different types of molecules, complexes and particles along a size continuum, including hydrated ions and other simple inorganic complexes, primarily organic complexes, primarily inorganic particles, and the inorganic elemental composition of individual particles. However, although online coupling can provide significant information by aligning the analysis time of a UV spectrophotometer in the AF4 detector chain with that of the (sp)ICP-(TOF)MS, the incredible variety of potential organic-inorganic combinations for individual particles remains unmeasured. For example, under oxidizing conditions, iron can exist in the form of aquo complexes, complexes with organic material, amorphous ferrihydrites with organic coatings or embedded organic molecules, oxyhydroxides with various levels of organic material embedded or on their surface, or mineral forms such as hematite and goethite with some amount of embedded and surficial organic matter. Given that each of these forms and organic matter/Fe configurations may exhibit different behaviour with respect to their environmental roles such as bioaccessibility and facilitating TE mobility, particle-by-particle information about organic contributions and type of organic matter will be highly valuable. Although this can be partially achieved using techniques such as scanning/transmission electron microscopy (S/TEM), the high number and potential diversity of particles in NPS currently prevent the efficient measurement of their representative distributions, and bombardment with electrons transforms organic carbon into ash, which acts as a contaminant. Improved speed or automated techniques for locating and characterizing NNPs on S/TEM grids will improve the viability of these methods for characterizing NPS.

The size distribution and zeta potential of NNPs are important variables for improving our understanding of NPS behaviour; hence, combining AF4-UV-ICP-MS and (sp)ICP-(TOF)MS with light scattering is recommended. This is particularly useful for polydisperse samples in which light scattering measurements are heavily biased, requiring pre-separation using AF4. However, the limitations of zeta potential for assessing the stability of colloids and DLVO theory for NPS should be duly considered.<sup>182,183</sup> The combination of electrical FFF with AF4 to create EAF4 is useful for conducting zeta potential measurements as a function of size, while avoiding the limitations of light scattering.<sup>184</sup> Nanoparticle tracking analysis is also a promising technique for rapidly characterizing the size distribution of NPS if it cannot be determined online with a light-scattering detector or other means following separation using AF4.<sup>185</sup>

Despite the growing application of sc/spICP-(TOF)MS for single-cell applications, its combination with other types of instruments able to discriminate the complexity of populations based on cell-by-cell properties can find numerous applications in nano-ecotoxicology. For instance, the development of mass cytometry TOFMS and flow-cytometers with a large array of

excitation lasers and acquisition detectors has propelled the frontiers of cellular population distinction and classification, and more importantly identified effects or phenotype deviations within a sub-population.<sup>186</sup> In environmental sciences, the recent applications of these state-of-the-art flow cytometer instruments allowed the identification of species in periphyton (assemblages of microorganisms), and with an appropriate data analysis pipeline, they have been distinguished from plastic particles in a single analysis.<sup>187-189</sup> In a simpler way, the addition of a flow-through fluorescence analyzer upstream of spICP-MS provided major advances in relating exposure doses to cell integrity at the population level.<sup>190</sup> These recent advancements in combined or on-line detection strongly support the feasibility of attributing pulse events recorded by elemental analyzers to living (*e.g.* bacteria/phytoplankton) or non-living (*e.g.* NNP hetero-aggregates) particles, allowing the structure and composition of NPS to be linked to ecological effects.

In general, every analytical technique is impacted by limitations and biases, which is especially true for highly diverse and dynamic samples such as NPS. Hence, the combination of multiple techniques provides additional, and sometimes critical information, even when measuring the same variable. This feature of NPS is perhaps the most challenging aspect of relating their properties to their behaviour and functions, particularly when error is multiplied in the combination of numerous variables to describe a system; however, resolving properties as a function of size using AF4 and other FFF methods significantly improves our ability to understand NPS. The measurement of particle-by-particle properties in the inorganic fraction of NPS using (sp)ICP-(TOF)MS also greatly resolves the diversity of NPS. Combined with these methods, ongoing improvements in other areas of nanometrology, data processing, and new paradigms for connecting large numbers of NNPs to their properties and behaviour as NPS will continue to improve our nanoscale understanding of natural nanosystems, with the corresponding advancements in environmental nanobiogeochemistry.

## Data availability

The data that support the figures and tables in this manuscript exist as part of numerous research programs undertaken by the co-authors and/or their supervising entities, each with distinct licensing policies. The data are therefore not available in a single location but may be accessed by contacting the corresponding authors.

## Conflicts of interest

There are no conflicts of interest to declare.

## Acknowledgements

CWC, CC and SF gratefully acknowledge funding support from the Natural Sciences and Engineering Research Council of Canada (NSERC). VIS, RG and IAMW acknowledge support



from Swiss National Science Foundation Projects No. 175721, No 204174 and R'Equip 220412, and to Thibaut Cossart and Joao Santos for the EPS of phytoplankton used for AF4-ICP-MS analysis of mercury dual isotope binding. The authors gratefully acknowledge valuable feedback from Reviewers and the Editor, which has greatly improved the quality of this publication. The table of content graphic for this manuscript was created using BioRender. This graphic is available online under the account of Worms, I. (2025), at the BioRender website: <https://BioRender.com/rnz32kx>.

## Notes and references

- 1 C. Yan, Y. Sheng, M. Ju, C. Ding, Q. Li, Z. Luo, M. Ding and M. Nie, Relationship between the characterization of natural colloids and metal elements in surface waters, *Environ. Sci. Pollut. Res.*, 2020, **27**, 31872–31883.
- 2 J. Means and R. Wuayaratne, Role of natural colloids in the transport of hydrophobic pollutants, *Science*, 1982, **215**, 968–970.
- 3 D. Deb and S. Chakma, Colloid and colloid-facilitated contaminant transport in subsurface ecosystem—a concise review, *Int. J. Environ. Sci. Technol.*, 2023, **20**, 6955–6988.
- 4 S. Wagner, A. Gondikas, E. Neubauer, T. Hofmann and F. von der Kammer, Spot the difference: engineered and natural nanoparticles in the environment—release, behavior, and fate, *Angew. Chem., Int. Ed.*, 2014, **53**, 12398–12419.
- 5 S. T. Kim, H.-R. Cho, E. C. Jung, W. Cha, M.-H. Baik and S. Lee, Asymmetrical flow field-flow fractionation coupled with a liquid waveguide capillary cell for monitoring natural colloids in groundwater, *Appl. Geochem.*, 2017, **87**, 102–107.
- 6 C. W. Cuss, I. Grant-Weaver and W. Shotyk, AF4-ICPMS with the 300 Da membrane to resolve metal-bearing “colloids” <1 kDa: optimization, fractogram deconvolution, and advanced quality control, *Anal. Chem.*, 2017, **89**, 8027–8035.
- 7 M. D. Montaño, C. W. Cuss, H. M. Holliday, M. B. Javed, W. Shotyk, K. L. Sobocinski, T. Hofmann, F. von der Kammer and J. F. Ranville, Exploring nanogeochemical environments: new insights from single particle ICP-TOFMS and AF4-ICPMS, *ACS Earth Space Chem.*, 2022, **6**, 943–952.
- 8 M. Tharaud, L. Schlatt, P. Shaw and M. F. Benedetti, Nanoparticle identification using single particle ICP-ToF-MS acquisition coupled to cluster analysis. From engineered to natural nanoparticles, *J. Anal. At. Spectrom.*, 2022, **37**, 2042–2052.
- 9 M. Mansor, S. Drabesch, T. Bayer, A. Van Le, A. Chauhan, J. Schmidtmann, S. Peiffer and A. Kappler, Application of single-particle ICP-MS to determine the mass distribution and number concentrations of environmental nanoparticles and colloids, *Environ. Sci. Technol. Lett.*, 2021, **8**, 589–595.
- 10 E. Bolea, M. S. Jimenez, J. Perez-Arantegui, J. C. Vidal, M. Bakir, K. Ben-Jedou, A. C. Gimenez-Ingalaturre, D. Ojeda, C. Trujillo and F. Laborda, Analytical applications of single particle inductively coupled plasma mass spectrometry: a comprehensive and critical review, *Anal. Methods*, 2021, **13**, 2742–2795.
- 11 H. Karkee and A. Gundlach-Graham, Characterization and Quantification of Natural and Anthropogenic Titanium-Containing Particles Using Single-Particle ICP-TOFMS, *Environ. Sci. Technol.*, 2023, **57**, 14058–14070.
- 12 L. Hendriks, A. Gundlach-Graham and D. Günther, Analysis of inorganic nanoparticles by single-particle inductively coupled plasma time-of-flight mass spectrometry, *Chimia*, 2018, **72**, 221–221.
- 13 J. Chorover, R. Kretzschmar, F. Garcia-Pichel and D. L. Sparks, Soil biogeochemical processes within the critical zone, *Elements*, 2007, **3**, 321–326.
- 14 K. U. Totsche, W. Amelung, M. H. Gerzabek, G. Guggenberger, E. Klumpp, C. Knief, E. Lehndorff, R. Mikutta, S. Peth and A. Prechtel, Microaggregates in soils, *J. Plant Nutr. Soil Sci.*, 2018, **181**, 104–136.
- 15 V. Nischwitz, N. Gottselig, A. Missong, T. Meyn and E. Klumpp, Field flow fractionation online with ICP-MS as novel approach for the quantification of fine particulate carbon in stream water samples and soil extracts, *J. Anal. At. Spectrom.*, 2016, **31**, 1858–1868.
- 16 V. Nischwitz, N. Gottselig, A. Missong, E. Klumpp and M. Braun, Extending the capabilities of field flow fractionation online with ICP-MS for the determination of particulate carbon in latex and charcoal, *J. Anal. At. Spectrom.*, 2018, **33**, 1363–1371.
- 17 A. Missong, R. Bol, V. Nischwitz, J. Krüger, F. Lang, J. Siemens and E. Klumpp, Phosphorus in water dispersible-colloids of forest soil profiles, *Plant Soil*, 2018, **427**, 71–86.
- 18 G. Moradi, R. Bol, L. Trbojevic, A. Missong, R. Mörchen, B. Fuentes, S. M. May, E. Lehndorff and E. Klumpp, Contrasting depth distribution of colloid-associated phosphorus in the active and abandoned sections of an alluvial fan in a hyper-arid region of the Atacama Desert, *Glob. Planet. Change*, 2020, **185**, 103090.
- 19 C. Claveranne-Lamolère, G. Lespes, S. Dubascoux, J. Aupiais, F. Pointurier and M. Potin-Gautier, Colloidal transport of uranium in soil: Size fractionation and characterization by field-flow fractionation-multi-detection, *J. Chromatogr. A*, 2009, **1216**, 9113–9119.
- 20 V. Nischwitz, N. Gottselig and M. Braun, Preparative field flow fractionation for complex environmental samples: online detection by inductively coupled plasma mass spectrometry and offline detection by gas chromatography with flame ionization, *J. Chromatogr. A*, 2020, **1632**, 461581.
- 21 N. Siebers, E. Voggenreiter, P. Joshi, J. Rethemeyer and L. Wang, Synergistic relationships between the age of soil organic matter, Fe speciation, and aggregate stability in an arable Luvisol, *J. Plant Nutr. Soil Sci.*, 2024, **187**, 77–88.
- 22 L. Krause, E. Klumpp, I. Nofz, A. Missong, W. Amelung and N. Siebers, Colloidal iron and organic carbon control soil aggregate formation and stability in arable Luvisols, *Geoderma*, 2020, **374**, 114421.



23 N. Tang, S. Dultz, D. Gerth and E. Klumpp, Soil colloids as binding agents in the formation of soil microaggregates in wet-dry cycles: A case study for arable Luvisols under different management, *Geoderma*, 2024, **443**, 116830.

24 N. Tang, N. Siebers, P. Leinweber, K.-U. Eckhardt, S. Dultz, V. Nischwitz and E. Klumpp, Implications of free and occluded fine colloids for organic matter preservation in arable soils, *Environ. Sci. Technol.*, 2022, **56**, 14133–14145.

25 X. Jiang, A. Wulf, R. Bol and E. Klumpp, Phosphorus content in water extractable soil colloids over a 2000 years chronosequence of paddy-rice management in the Yangtze River Delta, China, *Geoderma*, 2023, **430**, 116296.

26 X. Sun, S. M. May, W. Amelung, N. Tang, D. Brill, F. Arenas-Díaz, D. Contreras, B. Fuentes, R. Bol and E. Klumpp, Water-dispersible colloids distribution along an alluvial fan transect in hyper-arid Atacama Desert, *Geoderma*, 2023, **438**, 116650.

27 Q. Zhang, R. Bol, W. Amelung, A. Missong, J. Siemens, I. Mulder, S. Willbold, C. Müller, A. W. Muniz and E. Klumpp, Water dispersible colloids and related nutrient availability in Amazonian Terra Preta soils, *Geoderma*, 2021, **397**, 115103.

28 L. Du, C. W. Cuss, M. Dyck, T. Noernberg and W. Shotyk, Size fractionation of dissolved ( $<0.45\text{ }\mu\text{m}$ ) trace elements from extracted soil with water and  $\text{CaCl}_2$  using AF4-UV-ICPMS to predict their bioavailability, *Geoderma*, 2023, **440**, 116686.

29 B. Bergen, J. Lemmens, C. Moens and E. Smolders, Colloids facilitate transport of cadmium and uranium in arable soils, which is undetected by suction cups in the field, *Eur. J. Soil Sci.*, 2024, **75**, e13480.

30 I. C. Regelink, A. Voegelin, L. Weng, G. F. Koopmans and R. N. Comans, Characterization of colloidal Fe from soils using field-flow fractionation and Fe K-edge X-ray absorption spectroscopy, *Environ. Sci. Technol.*, 2014, **48**, 4307–4316.

31 F. Loosli, Z. Yi, J. Wang and M. Baalousha, Improved extraction efficiency of natural nanomaterials in soils to facilitate their characterization using a multimethod approach, *Sci. Total Environ.*, 2019, **677**, 34–46.

32 L. Du, C. Cuss, M. Dyck, T. Noernberg and W. Shotyk, Size-resolved analysis of trace elements in the dissolved fraction ( $<0.45\text{ }\mu\text{m}$ ) of soil solutions using a novel lysimeter and asymmetrical flow field-flow fractionation coupled to ultraviolet absorbance and inductively coupled plasma mass spectrometry, *Can. J. Soil Sci.*, 2020, **100**, 381–392.

33 N. Kallay and S. Žalac, Stability of nanodispersions: a model for kinetics of aggregation of nanoparticles, *J. Colloid Interface Sci.*, 2002, **253**, 70–76.

34 N. Maximova and O. Dahl, Environmental implications of aggregation phenomena: current understanding, *Curr. Opin. Colloid Interface Sci.*, 2006, **11**, 246–266.

35 N. Kovalchuk and V. Starov, Aggregation in colloidal suspensions: Effect of colloidal forces and hydrodynamic interactions, *Adv. Colloid Interface Sci.*, 2012, **179**, 99–106.

36 C. Moens, D. Montalvo and E. Smolders, The concentration and size distribution of iron-rich colloids in pore waters are related to soil organic matter content and pore water calcium concentration, *Eur. J. Soil Sci.*, 2021, **72**, 2199–2214.

37 J. P. Gustafsson, I. Persson, D. B. Kleja and J. W. Van Schaik, Binding of iron (III) to organic soils: EXAFS spectroscopy and chemical equilibrium modeling, *Environ. Sci. Technol.*, 2007, **41**, 1232–1237.

38 C. Sjöstedt, I. Persson, D. Hesterberg, D. B. Kleja, H. Borg and J. P. Gustafsson, Iron speciation in soft-water lakes and soils as determined by EXAFS spectroscopy and geochemical modelling, *Geochim. Cosmochim. Acta*, 2013, **105**, 172–186.

39 A. R. Mermut and A. F. Cano, Baseline studies of the clay minerals society source clays: chemical analyses of major elements, *Clays Clay Miner.*, 2001, **49**, 381–386.

40 I. C. Regelink, L. Weng, G. F. Koopmans and W. H. Van Riemsdijk, Asymmetric flow field-flow fractionation as a new approach to analyse iron-(hydr) oxide nanoparticles in soil extracts, *Geoderma*, 2013, **202**, 134–141.

41 I. C. Regelink, L. Weng and W. H. van Riemsdijk, The contribution of organic and mineral colloidal nanoparticles to element transport in a podzol soil, *Appl. Geochem.*, 2011, **26**, S241–S244.

42 E. Spielman-Sun, K. Boye, D. Dwivedi, M. Engel, A. Thompson, N. Kumar and V. Noël, A Critical Look at Colloid Generation, Stability, and Transport in Redox-Dynamic Environments: Challenges and Perspectives, *ACS Earth Space Chem.*, 2024, **8**, 630–653.

43 P. Hu, Y. Zhang, J. Wang, Y. Du, Z. Wang, Q. Guo, Z. Pan, X. Ma, B. Planer-Friedrich and Y. Luo, Mobilization of colloid- and nanoparticle-bound arsenic in contaminated paddy soils during reduction and reoxidation, *Environ. Sci. Technol.*, 2023, **57**, 9843–9853.

44 X. Li, Z. Cao, Y. Du, Y. Zhang, J. Wang, X. Ma, P. Hu, Y. Luo and L. Wu, Multi-metal contaminant mobilizations by natural colloids and nanoparticles in paddy soils during reduction and reoxidation, *J. Hazard. Mater.*, 2024, **461**, 132684.

45 D. Said-Pullicino, B. Giannetta, B. Demeglio, A. Missong, N. Gottselig, M. Romani, R. Bol, E. Klumpp and L. Celi, Redox-driven changes in water-dispersible colloids and their role in carbon cycling in hydromorphic soils, *Geoderma*, 2021, **385**, 114894.

46 L. Gfeller, A. Weber, I. Worms, V. I. Slaveykova and A. Mestrot, Mercury mobility, colloid formation and methylation in a polluted Fluvisol as affected by manure application and flooding-draining cycle, *Biogeosciences*, 2021, **18**, 3445–3465.

47 G. Dublet, I. Worms, M. Frutschi, A. Brown, G. C. Zünd, B. Bartova, V. I. Slaveykova and R. Bernier-Latmani, Colloidal size and redox state of uranium species in the porewater of a pristine mountain wetland, *Environ. Sci. Technol.*, 2019, **53**, 9361–9369.

48 W. Cai, Y. Wang, Y. Feng, P. Liu, S. Dong, B. Meng, H. Gong and F. Dang, Extraction and quantification of nanoparticulate mercury in natural soils, *Environ. Sci. Technol.*, 2022, **56**, 1763–1770.



49 Z. Li, M. Hadioui and K. J. Wilkinson, Extraction of Silicon-Containing Nanoparticles from an Agricultural Soil for Analysis by Single Particle Sector Field and Time-of-Flight Inductively Coupled Plasma Mass Spectrometry, *Nanomaterials*, 2023, **13**, 2049.

50 K. Ding, S. Liang, C. Xie, Q. Wan, C. Jin, S. Wang, Y.-T. Tang, M. Zhang and R. Qiu, Discrimination and Quantification of Soil Nanoparticles by Dual-Analyte Single Particle ICP-QMS, *Anal. Chem.*, 2022, **94**, 10745–10753.

51 G. D. Bland, M. Battifarano, A. E. Pradas del Real, G. Sarret and G. V. Lowry, Distinguishing engineered TiO<sub>2</sub> nanomaterials from natural Ti nanomaterials in soil using spICP-TOFMS and machine learning, *Environ. Sci. Technol.*, 2022, **56**, 2990–3001.

52 J. Wielinski, X. Huang and G. V. Lowry, Characterizing the Stoichiometry of Individual Metal Sulfide and Phosphate Colloids in Soils, Sediments, and Industrial Processes by Inductively Coupled Plasma Time-of-Flight Mass Spectrometry, *Environ. Sci. Technol.*, 2024, **58**, 12113–12122.

53 B. Stolpe, M. Hassellöv, K. Andersson and D. R. Turner, High resolution ICPMS as an on-line detector for flow field-flow fractionation; multi-element determination of colloidal size distributions in a natural water sample, *Anal. Chim. Acta*, 2005, **535**, 109–121.

54 D. M. Mitrano, A. Barber, A. Bednar, P. Westerhoff, C. P. Higgins and J. F. Ranville, Silver nanoparticle characterization using single particle ICP-MS (SP-ICP-MS) and asymmetrical flow field flow fractionation ICP-MS (AF4-ICP-MS), *J. Anal. At. Spectrom.*, 2012, **27**, 1131.

55 M. Hassellöv, B. Lyvén, C. Haraldsson and W. Sirinawin, Determination of continuous size and trace element distribution of colloidal material in natural water by on-line coupling of flow field-flow fractionation with ICPMS, *Anal. Chem.*, 1999, **71**, 3497–3502.

56 M. Benedetti, J. Ranville, T. Allard, A. Bednar and N. Menguy, The iron status in colloidal matter from the Rio Negro, Brasil, *Colloids Surf. A*, 2003, **217**, 1–9.

57 A. Praetorius, A. Gundlach-Graham, E. Goldberg, W. Fabienke, J. Navratilova, A. Gondikas, R. Kaegi, D. Günther, T. Hofmann and F. Von Der Kammer, Single-particle multi-element fingerprinting (spMEF) using inductively-coupled plasma time-of-flight mass spectrometry (ICP-TOFMS) to identify engineered nanoparticles against the elevated natural background in soils, *Environ. Sci.: Nano*, 2017, **4**, 307–314.

58 L. E. Anderson, B. F. Trueman, D. W. Dunnington and G. A. Gagnon, Relative importance of organic-and iron-based colloids in six Nova Scotian lakes, *npj Clean Water*, 2021, **4**, 26.

59 I. Jreije, A. Azimzada, M. Hadioui and K. J. Wilkinson, Measurement of CeO<sub>2</sub> nanoparticles in natural waters using a high sensitivity, single particle ICP-MS, *Molecules*, 2020, **25**, 5516.

60 F. Wang, M. Tharaud and M. F. Benedetti, Advancing surface river water preparation for nanoparticle quantification and characterization using spICP-MS or spICP-ToF-MS, *Microchem. J.*, 2024, **203**, 110843.

61 I. A. Worms, H. E. Chmiel, J. Traber, N. Tofield-Pasche and V. I. Slaveykova, Dissolved organic matter and associated trace metal dynamics from river to lake, under ice-covered and ice-free conditions, *Environ. Sci. Technol.*, 2019, **53**, 14134–14143.

62 J.-L. Wang, E. Alasonati, M. Tharaud, A. Gelabert, P. Fisicaro and M. F. Benedetti, Flow and fate of silver nanoparticles in small French catchments under different land-uses: the first one-year study, *Water Res.*, 2020, **176**, 115722.

63 M. Baalousha, J. Wang, M. Erfani and E. Goharian, Elemental fingerprints in natural nanomaterials determined using SP-ICP-TOF-MS and clustering analysis, *Sci. Total Environ.*, 2021, **792**, 148426.

64 T. Saito, T. Hamamoto, T. Mizuno, T. Iwatsuki and S. Tanaka, Comparative study of granitic and sedimentary groundwater colloids by flow-field flow fractionation coupled with ICP-MS, *J. Anal. At. Spectrom.*, 2015, **30**, 1229–1236.

65 J. F. Ranville, M. J. Hendry, T. N. Reszat, Q. Xie and B. D. Honeyman, Quantifying uranium complexation by groundwater dissolved organic carbon using asymmetrical flow field-flow fractionation, *J. Contam. Hydrol.*, 2007, **91**, 233–246.

66 A. J. Goodman, A. Scircle, A. Kimble, W. Harris, B. Calvitti, D. Sirkis, L. Mathurin, V. Grassi, J. F. Ranville and A. J. Bednar, Critical metal geochemistry in groundwaters influenced by dredged material, *Sci. Total Environ.*, 2023, **884**, 163725.

67 C. Cuss, M. Donner, I. Grant-Weaver, T. Noernberg, R. Pelletier, R. Sinnatamby and W. Shotyk, Measuring the distribution of trace elements amongst dissolved colloidal species as a fingerprint for the contribution of tributaries to large boreal rivers, *Sci. Total Environ.*, 2018, **642**, 1242–1251.

68 C. Cuss, M. Ghotbzadeh, I. Grant-Weaver, M. Javed, T. Noernberg and W. Shotyk, Delayed mixing of iron-laden tributaries in large boreal rivers: Implications for iron transport, water quality and monitoring, *J. Hydrol.*, 2021, **597**, 125747.

69 M. Ghotbzadeh, C. Cuss, I. Grant-Weaver, A. Markov, T. Noernberg, A. Ulrich and W. Shotyk, Spatiotemporal variations of total and dissolved trace elements and their distributions amongst major colloidal forms along and across the lower Athabasca River, *J. Hydrol. Reg. Stud.*, 2022, **40**, 101029.

70 D. J. Burger, J. Vogel, A. M. Kooijman, R. Bol, E. de Rijke, J. Schoorl, A. Lücke and N. Gottselig, Colloidal catchment response to snowmelt and precipitation events differs in a forested headwater catchment, *Vadose Zone J.*, 2021, **20**, e20126.

71 N. Gottselig, W. Amelung, J. W. Kirchner, R. Bol, W. Eugster, S. J. Granger, C. Hernández-Crespo, F. Herrmann, J. J. Keizer and M. Korkiakoski, Elemental composition of natural nanoparticles and fine colloids in European forest stream waters and their role as phosphorus carriers, *Global Biogeochem. Cycles*, 2017, **31**, 1592–1607.



72 N. Gottselig, V. Nischwitz, T. Meyn, W. Amelung, R. Bol, C. Halle, H. Vereecken, J. Siemens and E. Klumpp, Phosphorus binding to nanoparticles and colloids in forest stream waters, *Vadose Zone J.*, 2017, **16**, 1–12.

73 I. Lynch, K. A. Dawson, J. R. Lead and E. Valsami-Jones, in *Frontiers of nanoscience*, Elsevier, 2014, vol. 7, pp. 127–156.

74 J. Jiménez-Lamana and V. I. Slaveykova, Silver nanoparticle behaviour in lake water depends on their surface coating, *Sci. Total Environ.*, 2016, **573**, 946–953.

75 H. Xu, E. M. Houghton, C. J. Houghton and L. Guo, Variations in size and composition of colloidal organic matter in a negative freshwater estuary, *Sci. Total Environ.*, 2018, **615**, 931–941.

76 H. Lin and L. Guo, Variations in colloidal DOM composition with molecular weight within individual water samples as characterized by flow field-flow fractionation and EEM-PARAFAC analysis, *Environ. Sci. Technol.*, 2020, **54**, 1657–1667.

77 J. Yang, P. Tan, T. Huang and V. Nischwitz, Exploring the upper particle size limit for field flow fractionation online with ICP-MS to address the challenges of water samples from the Taihu Lake, *Anal. Chim. Acta*, 2020, **1093**, 16–27.

78 A. I. Ivaneev, S. Faucher, M. S. Ermolin, V. K. Karandashev, P. S. Fedotov and G. Lespes, Separation of nanoparticles from polydisperse environmental samples: comparative study of filtration, sedimentation, and coiled tube field-flow fractionation, *Anal. Bioanal. Chem.*, 2019, **411**, 8011–8021.

79 F. Loosli, Z. Yi, J. Wang and M. Baalousha, Dispersion of natural nanomaterials in surface waters for better characterization of their physicochemical properties by AF4-ICP-MS-TEM, *Sci. Total Environ.*, 2019, **682**, 663–672.

80 Y. Wang, C. Cuss and W. Shotyk, Application of asymmetric flow field-flow fractionation to the study of aquatic systems: coupled methods, challenges, and future needs, *J. Chromatogr. A*, 2020, **1632**, 461600.

81 I. A. Worms and V. I. Slaveykova, Asymmetrical flow field-flow fractionation coupled to ICP-MS for characterization of trace metal species in the environment from macromolecular to nano-assemblage forms: current challenges for quantification, *Chimia*, 2022, **76**, 34–44.

82 E. Neubauer, S. J. Köhler, F. Von Der Kammer, H. Laudon and T. Hofmann, Effect of pH and Stream Order on Iron and Arsenic Speciation in Boreal Catchments, *Environ. Sci. Technol.*, 2013, **47**, 7120–7128.

83 A. Hartland, J. R. Larsen, M. S. Andersen, M. Baalousha and D. O'Carroll, Association of arsenic and phosphorus with iron nanoparticles between streams and aquifers: implications for arsenic mobility, *Environ. Sci. Technol.*, 2015, **49**, 14101–14109.

84 E. K. Lesher, J. F. Ranville and B. D. Honeyman, Analysis of pH Dependent Uranium(VI) Sorption to Nanoparticulate Hematite by Flow Field-Flow Fractionation - Inductively Coupled Plasma Mass Spectrometry, *Environ. Sci. Technol.*, 2009, **43**, 5403–5409.

85 S. Harguindeguy, P. Crançon, M. Potin Gautier, F. Pointurier and G. Lespes, Colloidal mobilization from soil and transport of uranium in (sub)-surface waters, *Environ. Sci. Pollut. Res.*, 2019, **26**, 5294–5304.

86 N. Gottselig, J. Sohrt, D. Uhlig, V. Nischwitz, M. Weiler and W. Amelung, Groundwater controls on colloidal transport in forest stream waters, *Sci. Total Environ.*, 2020, **717**, 134638.

87 X.-R. Liu, W.-S. Liu, M. Zhang, C. Jin, K.-B. Ding, A. J. Baker, R.-L. Qiu, Y.-T. Tang and S.-Z. Wang, Organic-mineral colloids regulate the migration and fractionation of rare earth elements in groundwater systems impacted by ion-adsorption deposits mining in South China, *Water Res.*, 2024, **256**, 121582.

88 C. W. Cuss, C. N. Glover, M. B. Javed, A. Nagel and W. Shotyk, Geochemical and biological controls on the ecological relevance of total, dissolved, and colloidal forms of trace elements in large boreal rivers: review and case studies, *Environ. Rev.*, 2020, **28**, 138–163.

89 G. Lespes, S. Faucher and V. I. Slaveykova, Natural nanoparticles, anthropogenic nanoparticles, where is the frontier?, *Front. Environ. Sci.*, 2020, **8**, 71.

90 M. M. Nabi, J. Wang, M. Meyer, M.-N. Croteau, N. Ismail and M. Baalousha, Concentrations and size distribution of TiO<sub>2</sub> and Ag engineered particles in five wastewater treatment plants in the United States, *Sci. Total Environ.*, 2021, **753**, 142017.

91 F. Loosli, J. Wang, M. Sikder, K. Afshinnia and M. Baalousha, Analysis of engineered nanomaterials (Ag, CeO<sub>2</sub> and Fe<sub>2</sub>O<sub>3</sub>) in spiked surface waters at environmentally relevant particle concentrations, *Sci. Total Environ.*, 2020, **715**, 136927.

92 B. Stolpe, L. Guo, A. M. Shiller and M. Hassellöv, Size and composition of colloidal organic matter and trace elements in the Mississippi River, Pearl River and the northern Gulf of Mexico, as characterized by flow field-flow fractionation, *Mar. Chem.*, 2010, **118**, 119–128.

93 E. Maria, P. Crançon, P. Le Coustumer, M. Bridoux and G. Lespes, Comparison of preconcentration methods of the colloidal phase of a uranium-containing soil suspension, *Talanta*, 2020, **208**, 120383.

94 E. Maria, S. Faucher, P. Crançon and G. Lespes, Centrifugal ultrafiltration preconcentration for studying the colloidal phase of a uranium-containing soil suspension, *J. Chromatogr. A*, 2021, **1640**, 461957.

95 A. M. de Andrade, A. de Barros, I. O. Mazali and M. A. Z. Arruda, Fractionation and preconcentration of silver nanoparticles at environmentally relevant concentrations through induced eco-corona formation and spICP-MS characterization, *Environ. Sci.: Nano*, 2024, **11**, 1559–1570.

96 V. Kinnunen, S. Perämäki and R. Matilainen, Solid phase extraction materials as a key for improving the accuracy of silver nanoparticle characterization with single-particle inductively coupled plasma mass spectrometry in natural waters through dissolved silver removal, *Spectrochim. Acta, Part B*, 2022, **193**, 106431.

97 K.-B. Yoo, S. Yang, H. Choi and B.-T. Lee, Ion-exchange resins improve the analysis of metal nanoparticles in wastewater



using single-particle inductively coupled plasma-mass spectrometry, *Environ. Sci. Pollut. Res.*, 2024, **31**, 53090–53099.

98 L. Fréchette-Viens, M. Hadioui and K. J. Wilkinson, Quantification of ZnO nanoparticles and other Zn containing colloids in natural waters using a high sensitivity single particle ICP-MS, *Talanta*, 2019, **200**, 156–162.

99 K. Phalyvong, Y. Sivry, H. Pauwels, A. Gélabert, M. Tharaud, G. Wille, X. Bourrat, J. F. Ranville and M. F. Benedetti, Assessing CeO<sub>2</sub> and TiO<sub>2</sub> nanoparticle concentrations in the Seine River and its tributaries near Paris, *Front. Environ. Sci.*, 2021, **8**, 549896.

100 R. Gonzalez de Vega, T. E. Lockwood, X. Xu, C. Gonzalez de Vega, J. Scholz, M. Horstmann, P. A. Doble and D. Clases, Analysis of Ti-and Pb-based particles in the aqueous environment of Melbourne (Australia) via single particle ICP-MS, *Anal. Bioanal. Chem.*, 2022, **414**, 5671–5681.

101 J.-L. Wang, E. Alasonati, P. Fisicaro and M. F. Benedetti, Titanium nanoparticles fate in small-sized watersheds under different land-uses, *J. Hazard. Mater.*, 2022, **422**, 126695.

102 M. M. Nabi, J. Wang, E. Goharian and M. Baalousha, Temporal variation in TiO<sub>2</sub> engineered particle concentrations in the Broad River during dry and wet weathers, *Sci. Total Environ.*, 2022, **807**, 151081.

103 Q. V. Ly, T. Maqbool, Z. Zhang, Q. Van Le, X. An, Y. Hu, J. Cho, J. Li and J. Hur, Characterization of dissolved organic matter for understanding the adsorption on nanomaterials in aquatic environment: A review, *Chemosphere*, 2021, **269**, 128690.

104 X. Yang, Z. Wang, J. Xu, C. Zhang, P. Gao and L. Zhu, Effects of dissolved organic matter on the environmental behavior and toxicity of metal nanomaterials: A review, *Chemosphere*, 2024, **358**, 142208.

105 K. M. Kuhn, P. A. Maurice, E. Neubauer, T. Hofmann and F. von der Kammer, Accessibility of Humic-Associated Fe to a Microbial Siderophore: Implications for Bioavailability, *Environ. Sci. Technol.*, 2014, **48**, 1015–1022.

106 W. Liu, I. A. Worms, N. Herlin-Boime, D. Truffier-Boutry, I. Michaud-Soret, E. Mintz, C. Vidaud and F. Rollin-Genetet, Interaction of silver nanoparticles with metallothionein and ceruloplasmin: impact on metal substitution by Ag (i), corona formation and enzymatic activity, *Nanoscale*, 2017, **9**, 6581–6594.

107 W. Liu, I. Worms and V. I. Slaveykova, Interaction of silver nanoparticles with antioxidant enzymes, *Environ. Sci.: Nano*, 2020, **7**, 1507–1517.

108 M. Marchioni, T. Gallon, I. Worms, P.-H. Jouneau, C. Lebrun, G. Veronesi, D. Truffier-Boutry, E. Mintz, P. Delangle, A. Deniaud and I. Michaud-Soret, Insights into polythiol-assisted AgNP dissolution induced by bio-relevant molecules, *Environ. Sci.: Nano*, 2018, **5**, 1911–1920.

109 M. Marchioni, G. Veronesi, I. Worms, W. L. Ling, T. Gallon, D. Leonard, C. Gateau, M. Chevallet, P.-H. Jouneau, L. Carlini, C. Battocchio, P. Delangle, I. Michaud-Soret and A. Deniaud, Safer-by-design biocides made of tri-thiol bridged silver nanoparticle assemblies, *Nanoscale Horiz.*, 2020, **5**, 507–513.

110 I. Worms, D. F. Simon, C. S. Hassler and K. J. Wilkinson, Bioavailability of trace metals to aquatic microorganisms: importance of chemical, biological and physical processes on biouptake, *Biochimie*, 2006, **88**, 1721–1731.

111 T. Cossart, J. Garcia-Calleja, J. P. Santos, E. L. Kalahroodi, I. A. M. Worms, Z. Pedrero, D. Amouroux and V. I. Slaveykova, Role of phytoplankton in aquatic mercury speciation and transformations, *Environ. Chem.*, 2022, **19**, 104–115.

112 V. I. Slaveykova, M. Li, I. A. Worms and W. Liu, When environmental chemistry meets ecotoxicology: Bioavailability of inorganic nanoparticles to phytoplankton, *Chimia*, 2020, **74**, 115.

113 W. Liu, I. A. Worms, Ž. Jakšić and V. I. Slaveykova, Aquatic organisms modulate the bioreactivity of engineered nanoparticles: focus on biomolecular corona, *Front. Toxicol.*, 2022, **4**, 933186.

114 R. Gasco, I. A. Worms, A. Kantarcıyan and V. I. Slaveykova, Diatom-derived extracellular polymeric substances form eco-corona and enhance stability of silver nanoparticles, *Environ. Sci.: Nano*, 2024, **11**, 4138–4150.

115 I. Aharchaou, J. Py, S. Cambier, J. Loizeau, G. Cornelis, P. Rousselle, E. Battaglia and D. A. Vignati, Chromium hazard and risk assessment: New insights from a detailed speciation study in a standard test medium, *Environ. Toxicol. Chem.*, 2018, **37**, 983–992.

116 H. Dong, L. Liu, Q. Zhou, Y. Tang, H. Wang, Y. Yin, J. Shi, B. He, Y. Li, L. Hu and G. Jiang, Transformation of Mercuric Ions to Mercury Nanoparticles in Diatom *Chaetoceros curvisetus*, *Environ. Sci. Technol.*, 2023, **57**, 19772–19781.

117 K. El Hanafi, B. Gomez-Gomez, Z. Pedrero, P. Bustamante, Y. Cherel, D. Amouroux and Y. Madrid, Simple and rapid formic acid sample treatment for the isolation of HgSe nanoparticles from animal tissues, *Anal. Chim. Acta*, 2023, **1250**, 340952.

118 L. Paton, T. T. Moro, T. Lockwood, T. de Andrade Maranhão, G. Gössler, D. Clases and J. Feldmann, AF4-MALS-SP ICP-ToF-MS analysis gives insight into nature of HgSe nanoparticles formed by cetaceans, *Environ. Sci.: Nano*, 2024, **11**, 1883–1890.

119 R. Gasco, I. A. Worms, D. Santos and V. I. Slaveykova, Asymmetric flow field-flow fractionation for comprehensive characterization of hetero-aggregates made of nano-silver and extracellular polymeric substances, *J. Chromatogr. A*, 2025, **1739**, 465507.

120 A. B. S. da Silva and M. A. Z. Arruda, Single-cell ICP-MS to address the role of trace elements at a cellular level, *J. Trace Elem. Med. Biol.*, 2023, **75**, 127086.

121 M. Corte-Rodríguez, R. Álvarez-Fernández, P. García-Cancela, M. Montes-Bayón and J. Bettmer, Single cell ICP-MS using on line sample introduction systems: current developments and remaining challenges, *TrAC, Trends Anal. Chem.*, 2020, **132**, 116042.

122 S. Theiner, K. Loehr, G. Koellensperger, L. Mueller and N. Jakubowski, Single-cell analysis by use of ICP-MS, *J. Anal. At. Spectrom.*, 2020, **35**, 1784–1813.



123 R. C. Merrifield, C. Stephan and J. R. Lead, Quantification of Au Nanoparticle Biouptake and Distribution to Freshwater Algae Using Single Cell – ICP-MS, *Environ. Sci. Technol.*, 2018, **52**, 2271–2277.

124 B. Gomez-Gomez, M. Corte-Rodríguez, M. T. Perez-Corona, J. Bettmer, M. Montes-Bayón and Y. Madrid, Combined single cell and single particle ICP-TQ-MS analysis to quantitatively evaluate the uptake and biotransformation of tellurium nanoparticles in bacteria, *Anal. Chim. Acta*, 2020, **1128**, 116–128.

125 Y. Tanaka, R. Iida, S. Takada, T. Kubota, M. Yamanaka, N. Sugiyama, Y. Abdelnour and Y. Ogra, Quantitative Elemental Analysis of a Single Cell by Using Inductively Coupled Plasma-Mass Spectrometry in Fast Time-Resolved Analysis Mode, *ChemBioChem*, 2020, **21**, 3266–3272.

126 M. Amor, M. Tharaud, A. Gélabert and A. Komeili, Single-cell determination of iron content in magnetotactic bacteria: implications for the iron biogeochemical cycle, *Environ. Microbiol.*, 2020, **22**, 823–831.

127 X. Tian, Y. Wang, T. Xu, Y. Guo, Y. Bi, Y. Liu, Y. Liang, W. Cui, Y. Liu and L. Hu, Bioconcentration of Inorganic and Methyl Mercury by Algae Revealed Using Dual-Mass Single-Cell ICP-MS with Double Isotope Tracers, *Environ. Sci. Technol.*, 2024, **58**, 7860–7869.

128 L. Hendriks, V. M. Kissling, T. Buerki-Thurnherr and D. M. Mitrano, Development of single-cell ICP-TOFMS to measure nanoplastics association with human cells, *Environ. Sci.: Nano*, 2023, **10**, 3439–3449.

129 L. Hendriks and D. M. Mitrano, Direct measurement of microplastics by carbon detection via single particle ICP-TOFMS in complex aqueous suspensions, *Environ. Sci. Technol.*, 2023, **57**, 7263–7272.

130 S. K. Lower, M. F. Hochella Jr and T. J. Beveridge, Bacterial recognition of mineral surfaces: nanoscale interactions between *Shewanella* and  $\alpha$ -FeOOH, *Science*, 2001, **292**, 1360–1363.

131 D. F. McLeish, A. E. Williams-Jones, O. V. Vasyukova, J. R. Clark and W. S. Board, Colloidal transport and flocculation are the cause of the hyperenrichment of gold in nature, *Proc. Natl. Acad. Sci. U. S. A.*, 2021, **118**, e2100689118.

132 M. F. Hochella, There's plenty of room at the bottom: nanoscience in geochemistry, *Geochim. Cosmochim. Acta*, 2002, **66**, 735–743.

133 L. Petrella, N. Thébaud, D. Fougerouse, K. Evans, Z. Quadir and C. Laflamme, Colloidal gold transport: A key to high-grade gold mineralization?, *Miner. Deposita*, 2020, **55**, 1247–1254.

134 A. J. Goodman, M. E. Doherty and J. F. Ranville, Investigating nanoparticle pathfinder geochemistry in stream sediments using single-particle ICP-MS: a case study at the Sundance gold mineralization, Wyoming USA, *Geochem.: Explor., Environ., Anal.*, 2025, geochem2024-066.

135 A. J. Goodman and J. F. Ranville, Single particle inductively coupled plasma mass spectrometry: a new method to detect geochemical anomalies in stream sediments, *J. Geochem. Explor.*, 2023, **251**, 107231.

136 A. Goodman, H. Karkee, S. Huang, K. Pfaff, Y. D. Kuiper, Z. Chang, A. Gundlach-Graham and J. Ranville, Analysis of nano-mineral chemistry with single particle ICP-Time-of-Flight-MS; a novel approach to discriminate between geological environments, *Chem. Geol.*, 2024, 122498.

137 O. P. Missen, S. J. Mills, T. T. Moro, E. E. Villalobos-Portillo, H. Castillo-Michel, T. E. Lockwood, R. G. De Vega and D. Clases, Natural cobalt–manganese oxide nanoparticles: speciation, detection and implications for cobalt cycling, *Environ. Chem.*, 2024, **21**, EN23093.

138 S. E. Szakas and A. Gundlach-Graham, Isotopic ratio analysis of individual sub-micron particles via spICP-TOFMS, *J. Anal. At. Spectrom.*, 2024, **39**, 1874–1884.

139 B. T. Manard, V. C. Bradley, L. Hendriks, D. R. Dunlap, N. A. Zirakparvar, B. W. Ticknor, M. Toro-Gonzalez and H. B. Andrews, Isotopic analysis of Nd nanoparticles using single particle MC-ICP-MS: A comparative study with single particle-ICP-TOF-MS, *Talanta*, 2025, **286**, 127516.

140 D. Vantelon, M. Davranche, R. Marsac, C. La Fontaine, H. Guénet, J. Jfestin, G. Campaore, A. Beauvois and V. Briois, Iron speciation in iron–organic matter nanoaggregates: a kinetic approach coupling Quick-EXAFS and MCR-ALS chemometrics, *Environ. Sci.: Nano*, 2019, **6**, 2641–2651.

141 A. Gundlach-Graham, L. Hendriks, K. Mehrabi and D. Günther, Monte Carlo simulation of low-count signals in time-of-flight mass spectrometry and its application to single-particle detection, *Anal. Chem.*, 2018, **90**, 11847–11855.

142 A. Gundlach-Graham and R. Lancaster, Mass-dependent critical value expressions for particle finding in single-particle ICP-tofms, *Anal. Chem.*, 2023, **95**, 5618–5626.

143 F. Laborda, A. C. Giménez-Ingalaturre, E. Bolea and J. R. Castillo, About detectability and limits of detection in single particle inductively coupled plasma mass spectrometry, *Spectrochim. Acta, Part B*, 2020, **169**, 105883.

144 X. Tian, H. Jiang, L. Hu, M. Wang, W. Cui, J. Shi, G. Liu, Y. Yin, Y. Cai and G. Jiang, Simultaneous multi-element and multi-isotope detection in single-particle ICP-MS analysis: Principles and applications, *TrAC, Trends Anal. Chem.*, 2022, **157**, 116746.

145 I. A. Worms, K. Kavanagh, E. Moulin, N. Regier and V. I. Slaveykova, Asymmetrical flow field-flow fractionation methods for quantitative determination and size characterization of thiols and for mercury size speciation analysis in organic matter-rich natural waters, *Front. Chem.*, 2022, **10**, 800696.

146 A. H. Henke, K. Flores, A. J. Goodman, K. Magurany, K. LeVanseler, J. Ranville, J. L. Gardea-Torresdey and P. K. Westerhoff, Interlaboratory comparison of centrifugal ultrafiltration with ICP-MS detection in a first-step towards methods to screen for nanomaterial release during certification of drinking water contact materials, *Sci. Total Environ.*, 2024, **912**, 168686.

147 I. Jreije, M. Hadioui and K. J. Wilkinson, Sample preparation for the analysis of nanoparticles in natural waters by single particle ICP-MS, *Talanta*, 2022, **238**, 123060.



148 G. D. Bland and G. V. Lowry, Multistep method to extract moderately soluble copper oxide nanoparticles from soil for quantification and characterization, *Anal. Chem.*, 2020, **92**, 9620–9628.

149 T. R. Holbrook, D. Gallot-Duval, T. Reemtsma and S. Wagner, An investigation into LA-spICP-ToF-MS uses for in situ measurement of environmental multi-elemental nanoparticles, *J. Anal. At. Spectrom.*, 2021, **36**, 2107–2115.

150 R. L. Buckman and A. Gundlach-Graham, Machine learning analysis to classify nanoparticles from noisy spICP-TOFMS data, *J. Anal. At. Spectrom.*, 2023, **38**, 1244–1252.

151 I. A. Worms, J. Traber, D. Kistler, L. Sigg and V. I. Slaveykova, Uptake of Cd (II) and Pb (II) by microalgae in presence of colloidal organic matter from wastewater treatment plant effluents, *Environ. Pollut.*, 2010, **158**, 369–374.

152 I. A. Worms, D. Adenmatten, P. Miéville, J. Traber and V. I. Slaveykova, Photo-transformation of pedogenic humic acid and consequences for Cd (II), Cu (II) and Pb (II) speciation and bioavailability to green microalga, *Chemosphere*, 2015, **138**, 908–915.

153 A. H. Nagel, C. W. Cuss, G. G. Goss, W. Shotyk and C. N. Glover, The effect of major ions and dissolved organic matter on complexation and toxicity of dissolved thallium to *Daphnia magna*, *Environ. Toxicol. Chem.*, 2019, **38**, 2472–2479.

154 M. L. Wells and E. D. Goldberg, Occurrence of small colloids in sea water, *Nature*, 1991, **353**, 342–344.

155 V. Barrón and J. Torrent, in *Minerals at the Nanoscale*, ed. F. Nieto, K. J. T. Livi and R. Oberti, Mineralogical Society of Great Britain and Ireland, 2013.

156 G. R. Aiken, H. Hsu-Kim and J. N. Ryan, Influence of Dissolved Organic Matter on the Environmental Fate of Metals, Nanoparticles, and Colloids, *Environ. Sci. Technol.*, 2011, **45**, 3196–3201.

157 C. A. Silvera Batista, R. G. Larson and N. A. Kotov, Nonadditivity of nanoparticle interactions, *Science*, 2015, **350**, 1242477.

158 M. Antonietti and C. Göltner, Superstructures of functional colloids: chemistry on the nanometer scale, *Angew. Chem., Int. Ed. Engl.*, 1997, **36**, 910–928.

159 J. Dobnikar, M. Brunner, H.-H. von Grünberg and C. Bechinger, Three-body interactions in colloidal systems, *Phys. Rev. E: Stat., Nonlinear, Soft Matter Phys.*, 2004, **69**, 031402.

160 E. Bormashenko, A. A. Fedorets, M. Frenkel, L. A. Dombrovsky and M. Nosonovsky, Clustering and self-organization in small-scale natural and artificial systems, *Philos. Trans. R. Soc., A*, 2020, **378**, 20190443.

161 R. H. Swendsen, Statistical mechanics of colloids and Boltzmann's definition of the entropy, *Am. J. Phys.*, 2006, **74**, 187–190.

162 L. Corté, S. J. Gerbode, W. Man and D. J. Pine, Self-organized criticality in sheared suspensions, *Phys. Rev. Lett.*, 2009, **103**, 248301.

163 S. Fortuna and A. Troisi, Agent-based modeling for the 2D molecular self-organization of realistic molecules, *J. Phys. Chem. B*, 2010, **114**, 10151–10159.

164 D. Frenkel, Why colloidal systems can be described by statistical mechanics: some not very original comments on the Gibbs paradox, *Mol. Phys.*, 2014, **112**, 2325–2329.

165 M. Nosonovsky and P. Roy, Scaling in colloidal and biological networks, *Entropy*, 2020, **22**, 622.

166 B. Tadić and R. Melnik, Self-organised critical dynamics as a key to fundamental features of complexity in physical, biological, and social networks, *Dynamics*, 2021, **1**, 181–197.

167 G. Campos-Villalobos, E. Boattini, L. Filion and M. Dijkstra, Machine learning many-body potentials for colloidal systems, *J. Chem. Phys.*, 2021, **155**, 174902.

168 J. O'Leary, R. Mao, E. J. Pretti, J. A. Paulson, J. Mittal and A. Mesbah, Deep learning for characterizing the self-assembly of three-dimensional colloidal systems, *Soft Matter*, 2021, **17**, 989–999.

169 S. Ouyang, X. Hu, Q. Zhou, X. Li, X. Miao and R. Zhou, Nanocolloids in Natural Water: Isolation, Characterization, and Toxicity, *Environ. Sci. Technol.*, 2018, **52**, 4850–4860.

170 D. A. Vignati, T. Dworak, B. Ferrari, B. Koukal, J.-L. Loizeau, M. Minouflet, M. I. Camusso, S. Polesello and J. Dominik, Assessment of the geochemical role of colloids and their impact on contaminant toxicity in freshwaters: An example from the Lambro- Po System (Italy), *Environ. Sci. Technol.*, 2005, **39**, 489–497.

171 H. Saeed, A. Hartland, N. J. Lehto, M. Baalousha, M. Sikder, D. Sandwell, M. Mucalo and D. P. Hamilton, Regulation of phosphorus bioavailability by iron nanoparticles in a monomictic lake, *Sci. Rep.*, 2018, **8**, 17736.

172 D. S. Smith, R. A. Bell and J. R. Kramer, Metal speciation in natural waters with emphasis on reduced sulfur groups as strong metal binding sites, *Comp. Biochem. Physiol., Part C: Toxicol. Pharmacol.*, 2002, **133**, 65–74.

173 D. S. Smith, R. Nasir, W. Parker, A. Peters, G. Merrington, R. van Egmond and S. Lofts, Developing understanding of the fate and behaviour of silver in fresh waters and waste waters, *Sci. Total Environ.*, 2021, **757**, 143648.

174 U. Ndu, G. A. Christensen, N. A. Rivera, C. M. Gionfriddo, M. A. Deshusses, D. A. Elias and H. Hsu-Kim, Quantification of mercury bioavailability for methylation using diffusive gradient in thin-film samplers, *Environ. Sci. Technol.*, 2018, **52**, 8521–8529.

175 S. Ouyang, Y. Li, T. Zheng, K. Wu, X. Wang and Q. Zhou, Ecotoxicity of natural nanocolloids in aquatic environment, *Water*, 2022, **14**, 2971.

176 J. Buffle, The key role of environmental colloids/nanoparticles for the sustainability of life, *Environ. Chem.*, 2006, **3**, 155–158.

177 C. Freeman, N. Fenner, N. Ostle, H. Kang, D. Dowrick, B. Reynolds, M. Lock, D. Sleep, S. Hughes and J. Hudson, Export of dissolved organic carbon from peatlands under elevated carbon dioxide levels, *Nature*, 2004, **430**, 195–198.

178 G. A. Weyhenmeyer, Y. T. Prairie and L. J. Tranvik, Browning of boreal freshwaters coupled to carbon-iron interactions along the aquatic continuum, *PLoS One*, 2014, **9**, e88104.



179 H. A. De Wit, S. Valinia, G. A. Weyhenmeyer, M. N. Futter, P. Kortelainen, K. Austnes, D. O. Hessen, A. Räike, H. Laudon and J. Vuorenmaa, Current browning of surface waters will be further promoted by wetter climate, *Environ. Sci. Technol. Lett.*, 2016, **3**, 430–435.

180 R. Krachler, R. F. Krachler, G. Wallner, P. Steier, Y. El Abiead, H. Wiesinger, F. Jirsa and B. K. Keppler, Sphagnum-dominated bog systems are highly effective yet variable sources of bio-available iron to marine waters, *Sci. Total Environ.*, 2016, **556**, 53–62.

181 A. Räike, A. Taskinen, L. H. Härkönen, P. Kortelainen and A. Lepistö, Browning from headwaters to coastal areas in the boreal region: Trends and drivers, *Sci. Total Environ.*, 2024, **927**, 171959.

182 E. M. Hotze, T. Phenrat and G. V. Lowry, Nanoparticle aggregation: challenges to understanding transport and reactivity in the environment, *J. Environ. Qual.*, 2010, **39**, 1909–1924.

183 S. Bhattacharjee, DLS and zeta potential—what they are and what they are not?, *J. Controlled Release*, 2016, **235**, 337–351.

184 C. L. Plavchak, W. C. Smith, C. R. M. Bria and S. K. R. Williams, New Advances and Applications in Field-Flow Fractionation, *Annu. Rev. Anal. Chem.*, 2021, **14**, 257–279.

185 J. A. Gallego-Urrea, J. Tuoriniemi, T. Pallander and M. Hassellöv, Measurements of nanoparticle number concentrations and size distributions in contrasting aquatic environments using nanoparticle tracking analysis, *Environ. Chem.*, 2010, **7**, 67–81.

186 A. Schäfer, S. M. D'Almeida, J. Dorier, N. Guex, J. Villard and M. Garcia, Comparative assessment of cytometry by time-of-flight and full spectral flow cytometry based on a 33-color antibody panel, *J. Immunol. Methods*, 2024, **527**, 113641.

187 L. Sgier, R. Freimann, A. Zupanic and A. Kroll, Flow cytometry combined with t-SNE for the analysis of microbial biofilms and detection of microplastics, *Nat. Commun.*, 2016, **7**, 11587.

188 X. Wang, Y. Li, A. Kroll and D. M. Mitrano, Differentiating Microplastics from Natural Particles in Aqueous Suspensions Using Flow Cytometry with Machine Learning, *Environ. Sci. Technol.*, 2024, **58**(23), 10240–10251.

189 S. N. Merbt, A. Kroll, M. Tamminen, P. A. Rühs, B. Wagner, L. Sgier, O. Sembalova, B. Abel, A. Tlili and K. Schirmer, Influence of microplastics on microbial structure, function, and mechanical properties of stream periphyton, *Front. Environ. Sci.*, 2022, **10**, 928247.

190 C. Wu, X. Wei, X. Men, X. Zhang, Y.-L. Yu, Z.-R. Xu, M.-L. Chen and J.-H. Wang, Two-Dimensional Cytometry Platform for Single-Particle/Cell Analysis with Laser-Induced Fluorescence and ICP-MS, *Anal. Chem.*, 2021, **93**, 8203–8209.

